Geochemical signals of carbonatite-related critical metals in provincial stream sediments

Alexei S. Rukhlov[1, a], Yao Cui[1], Quinn Cunningham[1], Gabe Fortin[1], and Cameron Anderson[1]

[1] British Columbia Geological Survey, Ministry of Energy, Mines and Low Carbon Innovation, Victoria, BC, V8W 9N3
[a] corresponding author: Alexei.Rukhlov@gov.bc.ca

Recommended citation: Rukhlov, A.S., Cui, Y., Cunningham, Q., Fortin, G., and Anderson, C., 2024. Geochemical signals of carbonatite-related critical metals in provincial stream sediments. In: Geological Fieldwork 2023, British Columbia Ministry of Energy, Mines and Low Carbon Innovation, British Columbia Geological Survey Paper 2024-01, pp. 97-122.

Abstract

Consisting of at least 30% primary carbonate minerals, carbonatites are rare igneous rocks that have become increasingly important exploration targets, because they are major sources of Nb, rare earth elements (REE), and other critical minerals. Demand for these minerals has rapidly increased as the world transitions to low-carbon technologies. The British Columbia alkaline province, which defines a long (at least 1000 km), narrow (ca. 200 km) orogen-parallel belt along the western flank of Ancestral North America, contains numerous carbonatites and related silica-undersaturated and alkaline silicate rocks that host REE and rare-metal resources. Using multi-element stream-sediment geochemical data collected as part of the Regional Geochemical Survey (RGS) program since 1976, we define a multivariant 'critical mineral index' to assess prospectivity for carbonatite-hosted critical metals. Based on discriminant analysis of a training sub-set of the data downstream of known carbonatite occurrences (n=26), our carbonatite index, which is validated by a test sub-set of the data (n=27), highlights numerous areas prospective for REE in the alkaline province. Stream-sediment data showing carbonatite index scores greater than the 93rd percentile (n=50) reveal maximum contrast of REE, Nb, Ta, Ti, Zr, Hf, Th, U, P, K and other carbonatite indicators relative to the median (background) concentrations in stream sediments of the study area. Estimated predicted geochemical resources (in tonnes of metal per 1 m depth), based on productivities of metals in the stream basins, suggest significant potential for REE and other carbonatite-hosted critical metals. Based on data from known carbonatites, we propose a refined prospectivity approach to assess the critical metals potential of underexplored regions that includes detailed stream-sediment, panned heavy mineral concentrate, and soil lithochemical surveys and high-resolution airborne radiometric and magnetic data.

Keywords: Carbonatite, alkaline rocks, regional geochemical survey (RGS), stream sediments, heavy mineral concentrate (HMC), drainage geochemistry, critical minerals, rare earth elements (REE), rare metals, niobium, tantalum, Blue River, Upper Fir, Aley, multivariate statistics, discriminant analysis, carbonatite index, predicted geochemical resources

1. Introduction

Reconnaissance geochemical surveys have a long history of supporting mineral exploration in underexplored regions of British Columbia. Regional sampling of stream sediments and waters has been carried out by mining companies since 1950s and was later adopted by the Geological Survey of Canada, the British Columbia Geological Survey, and Geoscience BC as part of the Regional Geochemical Survey (RGS) programs (Lett and Rukhlov, 2017). Interpretation of these data has led to the discovery of precious and base metal deposits such as the Highland Valley Copper mine and the Galore Creek proposed mine (e.g., Brummer et al., 1987).

Consisting of at least 30% primary carbonate minerals, carbonatites are rare igneous rocks that have become increasingly important exploration targets, because they are major sources of Nb, rare earth elements (REE), and other critical minerals needed as the world transitions to low-carbon technologies (Hickin et al., 2024). Although lithogeochemistry of panned heavy mineral concentrate (HMC) and indicator minerals of stream sediments have become established techniques for rare-metal and REE prospecting (e.g., Rukhlov and Gorham, 2007; Gorham, 2008; Gorham et al., 2009; Simandl et al., 2017) the application of regional geochemical surveys to carbonatite-hosted minerals has not been evaluated.

The British Columbia alkaline province, which defines a long (at least 1000 km), narrow (ca. 200 km) orogen-parallel belt along the western flank of Ancestral North America, contains numerous carbonatites and related silica-undersaturated and alkaline silicate rocks (Fig. 1). Some of these rocks host REE (e.g., Wicheeda; Dalsin et al., 2015; Trofanenko et al., 2016) and Ta-Nb (e.g., Aley; Mäder, 1987; Chakhmouradian et al., 2015; and Upper Fir; Rukhlov et al., 2018). This study evaluates multi-element stream-sediment geochemical data collected as part of the RGS program in the Omineca and Foreland morphotectonic belts for prospectivity indicators of carbonatite-hosted critical metals. We also consider examples of detailed surveys near known carbonatite occurrences in the Blue River area and at the Aley deposit (Fig. 2) to discuss applications of panned heavy-mineral concentrate and soil lithogeochemistry, high-resolution airborne radiometrics and magnetics, and productivities of carbonatite indicators in stream basins. Using these data, we define a multivariant 'critical mineral index' that can be used to

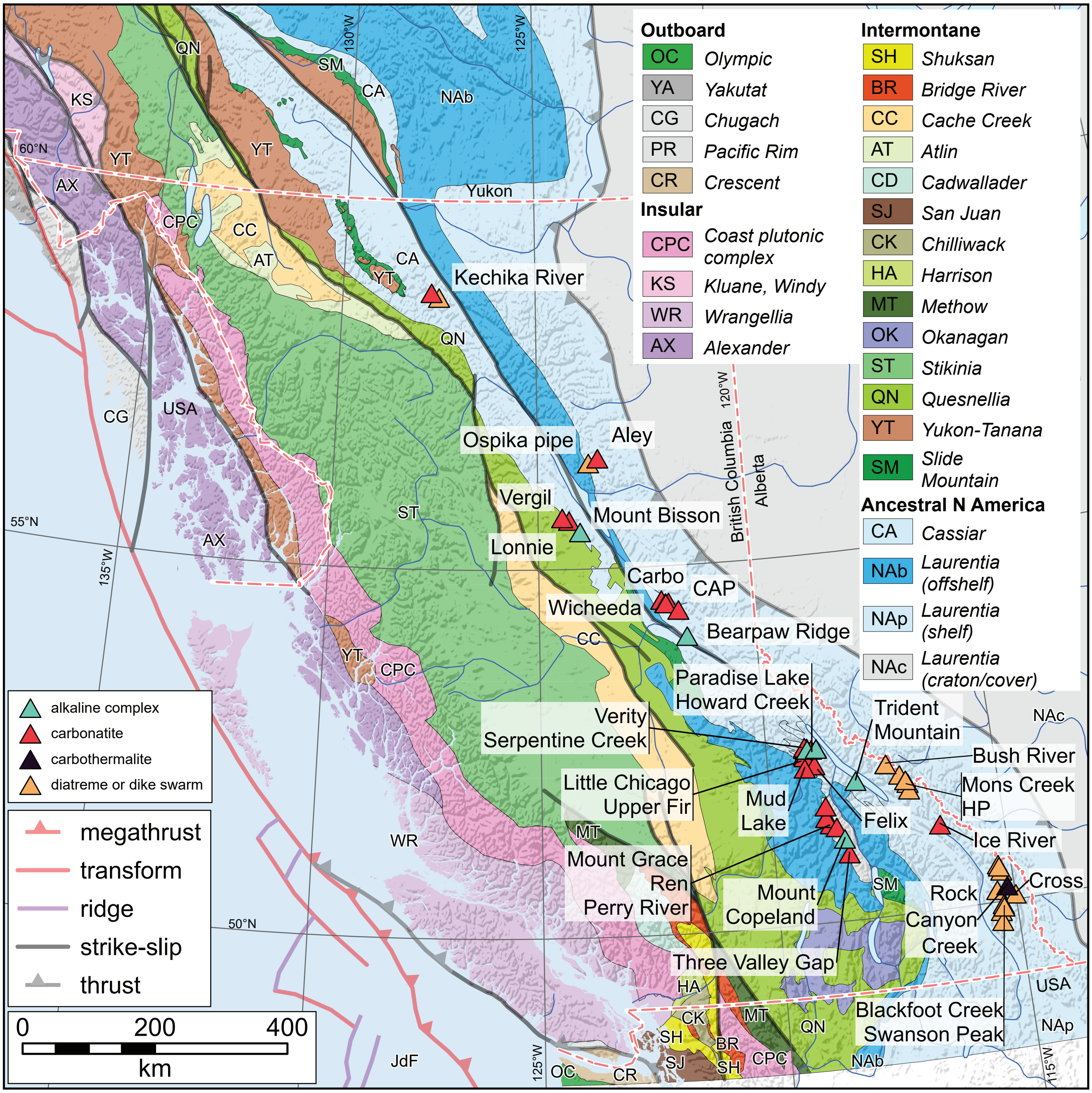

Fig. 1. Carbonatite and related-rock occurrences along the British Columbia alkaline province (after Höy, 1988; Parrish and Scammell, 1988; Pell, 1994; Millonig and Groat, 2013; Rukhlov et al., 2018). Terranes after Colpron (2020).

highlight prospective areas in the alkaline province and regions elsewhere that warrant prospecting for carbonatite-hosted commodities.

2. British Columbia carbonatites and related rocks

In the Canadian Cordillera, carbonatite and related ultramafic, silica-undersaturated and alkaline silicate bodies were emplaced episodically at ca. 810-700 Ma (Mount Copeland, Perry River, Ren), 500-400 Ma (Blackfoot Creek, Bush River, Felix, HP, Kechika River, Little Chicago, Mons Creek, Swanson Peak), and 360-320 Ma (Aley, Howard Creek, Ice River, Lonnie, Mount Grace, Mud Lake, Ospika, Paradise Lake, Serpentine Creek, Three Valley Gap, Upper Fir, Trident Mountain, Vergil, Verity, Wicheeda); the Cross kimberlite is 245 Ma. Collectively, these rocks form part of the British Columbia alkaline province (Fig. 1; Höy, 1988; Parrish and Scammell, 1988; Pell and Höy, 1989; Pell, 1994; Rukhlov and Bell, 2010; Millonig et al., 2012; Millonig and Groat, 2013;

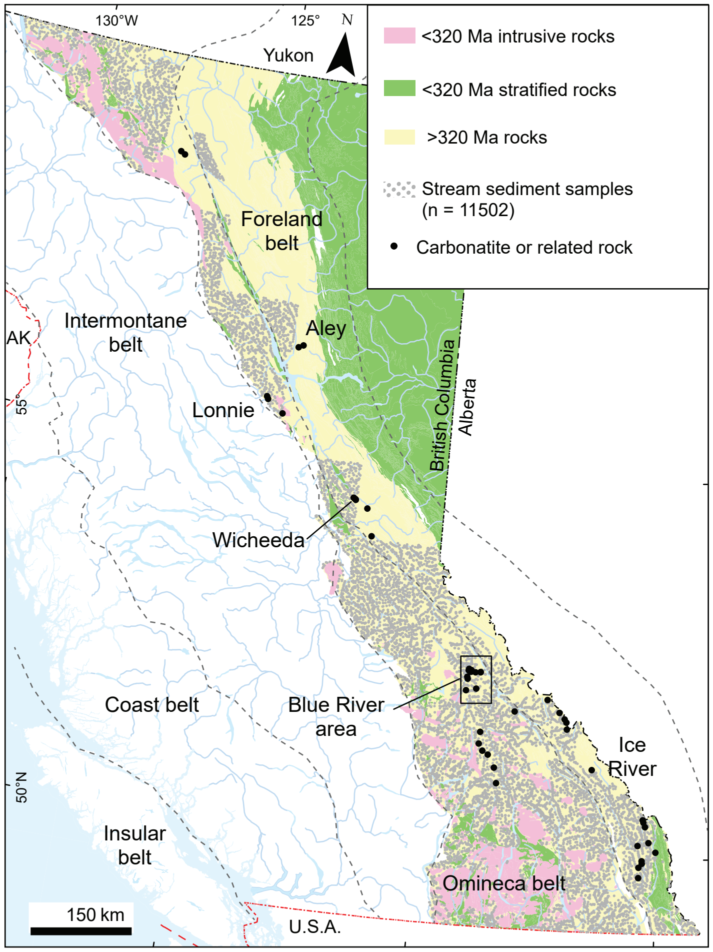

Fig. 2. Selected stream sediment samples in the study area (after Han and Rukhlov, 2017, 2020b). Carbonatite and related-rock occurrences after Höy (1988), Parrish and Scammell (1988), Pell (1994), Millonig and Groat (2013), and Rukhlov et al. (2018). Morphotectonic boundaries after Gabrielse et al. (1991). Geology from BC Digital Geology version 2021-12-19 (Cui et al., 2017).

Chakhmouradian et al., 2015; Mitchell et al., 2017; Rukhlov et al., 2018; McLeish and Johnston, 2019; McLeish et al., 2020; Burgess et al., 2023). The Neoproterozoic and early Paleozoic pulses of carbonatite and alkaline magmatism mark protracted breakup of the supercontinent Rodinia and subsequent passive margin development on the western flank of Laurentia (Li et al., 2008; Bond and Kominz, 1984; Ross, 1991; Colpron et al., 2002). The late Paleozoic carbonatite and alkaline complexes, which host Nb-Ta deposits (e.g., Upper Fir in the Blue River area and Aley) and REE deposits (e.g., Wicheeda), were injected near the continental margin while subduction was taking place to the west (Nelson et al., 2013).

Hosted by the parautochthonous rocks of the Omineca and Foreland belts (Fig. 2), carbonatites and related rocks range from intrusive complexes with a paucity of carbonatites (e.g., Trident Mountain, Mount Copeland) to carbonatite complexes with a paucity of silicate rocks (e.g., Aley, Blue River, Frenchman Cap). Both the carbonatites and host rocks experienced multiple episodes of deformation and metamorphism during Mesozoic and Cenozoic accretionary tectonics while outboard terranes welded to each other and to Laurentia (Scammell, 1987, 1993; Scammell and Brown, 1990; Pell, 1994; Millonig et al., 2013). Intrusive complexes made up of mainly silica-undersaturated and alkaline silicate rocks, such as the Ice River complex, form small (up to 29 km^2 at surface), compositionally zoned bodies that are circular to elongate to amoeboid in plan view (Dawson, 1886; Currie, 1975; Peterson and Currie, 1994). Associated ultramafic lamprophyres and REE-Sr-rich carbothermalite dikes are common, with the latter consisting of Mn-calcite, barytocalcite, and zeolite with minor strontianite, Nb-ilmenite, and REE-F-carbonates (Mumford, 2009; Brown, 2013). Carbonatites lacking associated contemporaneous silicate rocks typically form regional swarms of individual occurrences across areas of 1000 km^2 (e.g., Blue River; Pell, 1994; Mitchell et al., 2017; Rukhlov et al., 2018; Çimen et al., 2019).

3. Blue River area

In the Blue River area (Fig. 3), at least 18 carbonatite and two alkaline, silica-undersaturated-rock bodies are exposed, including at the Upper Fir deposit, one of the largest and best studied Nb-Ta occurrences in the Canadian Cordillera (Chudy, 2013; Rukhlov et al., 2018). Both Cambrian and late

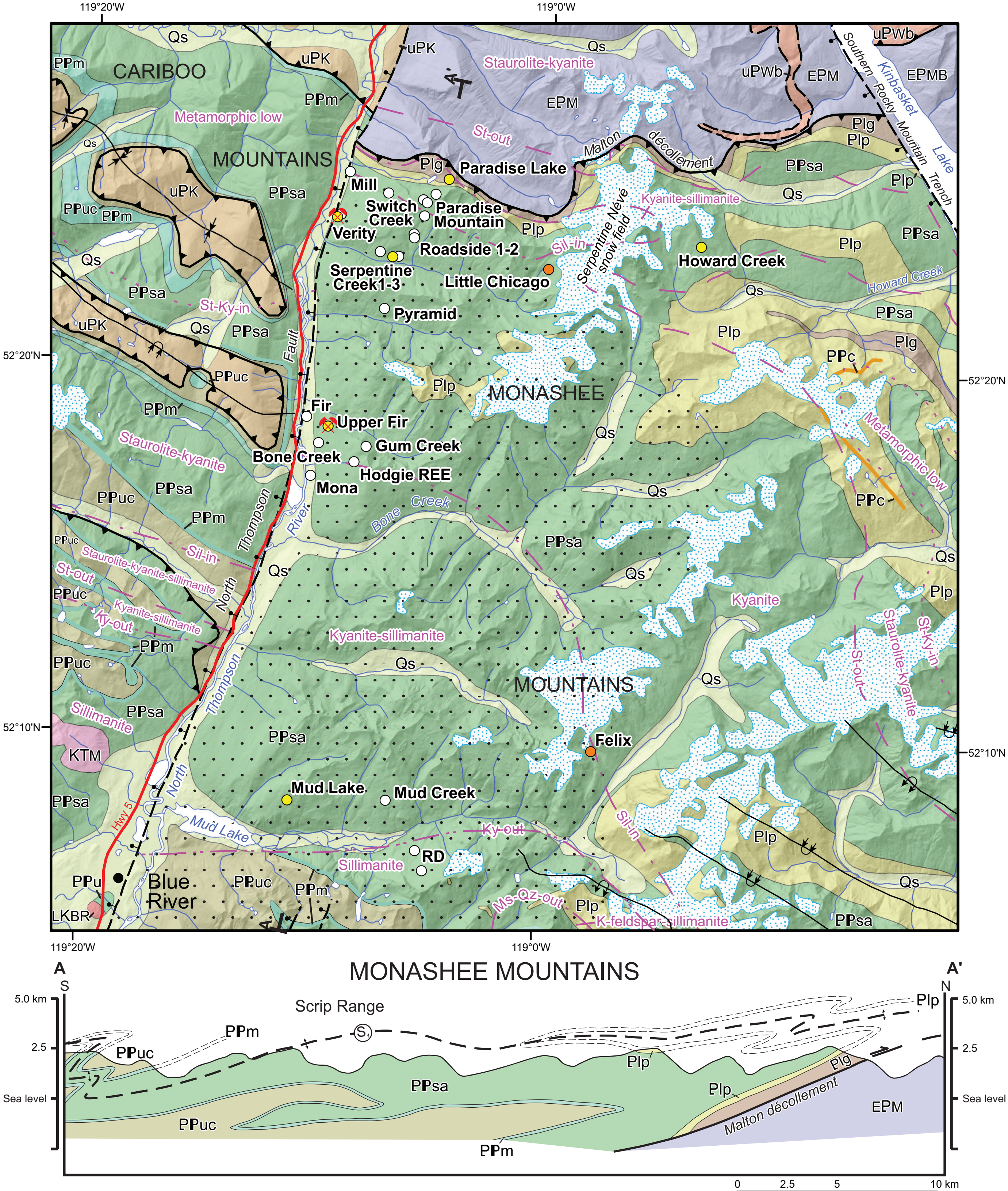

Fig. 3. Carbonatite and related-rock occurrences of the Blue River area (after Pell, 1994; Rukhlov and Bell, 2010; Millonig et al., 2012, 2013; Millonig and Groat, 2013; Rukhlov et al., 2018). Geology and metamorphic isograds after Campbell (1968), Simony et al. (1980), Raeside and Simony (1983), Pell and Simony (1987), McDonough and Murphy (1990), McDonough et al. (1991a, b, 1992), Digel et al. (1998), and Murphy (2007).

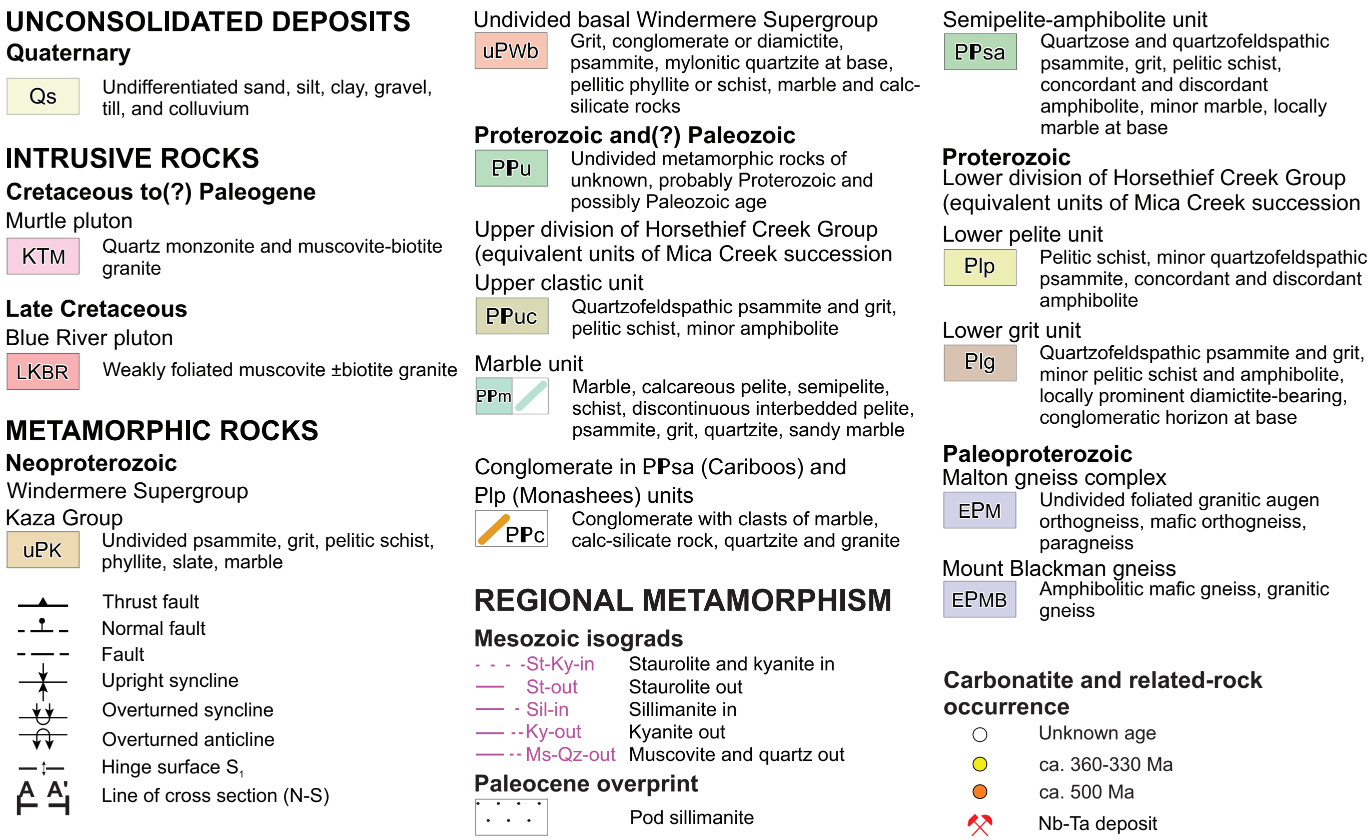

Fig. 3. Continued. Legend.

Paleozoic carbonatites made up of dolomite and calcite are hosted by metamorphosed Neoproterozoic pelitic, arenaceous, and amphibolitic rocks of the Mica Creek assemblage. Metamorphosed to amphibolite grade during Mesozoic to Cenozoic orogeny, the carbonatites form isoclinally folded, sill-like tabular bodies up to 72 m thick and display diverse fabrics, including coarse-grained, granoblastic to fine-grained, foliated, and porphyroclastic varieties. They contain 10-15 vol.% fluorapatite, 5-10 vol.% amphiboles, and variable amounts of olivine, chondrodite, clinopyroxene, phlogopite, magnetite, ilmenite, pyrrhotite, pyrite, pyrochlore supergroup, ferrocolumbite, fersmite, nyoboaeschynite, zircon, baddeleyite, zirconolite, and monazite (Rukhlov et al., 2018). The Upper Fir carbonatite contains an NI 43-101-compliant resource of 48.4 million tonnes (Indicated) grading 1610 ppm Nb_2O_5 and 197 ppm Ta_2O_5 plus 5.4 million tonnes (Inferred) averaging 1760 ppm Nb_2O_5 and 191 ppm Ta_2O_5 (Kulla and Hardy, 2015). Pyrochlore and ferrocolumbite are the main hosts of Nb and Ta (Chudy, 2013; Rukhlov et al., 2018). Molybdenite occurs in some carbonatites and related rocks, including alkali-rich metasomatic rocks such as fenites and glimmerites at Fir, Perry River, Mount Grace, Wicheeda, and the Mount Copeland past producer (Currie, 1976; White, 1982; Höy, 1988; Trofanenko et al., 2016; Rukhlov et al., 2018).

4. Rock, soil, and drainage lithogeochemical data from the Blue River area

In addition to distinct physical and mineralogical characteristics, carbonatites are readily distinguished from sedimentary carbonate rocks (Table 1) by their extremely high concentrations (up to 1000 times the average upper continental crust) of REE, rare metals, F, P, Sr, Ba, Th, U, and other elements (Fig. 4). Data from both provincial, reconnaissance-scale drainage surveys and detailed lithogeochemical drainage and soil surveys in the Blue River area (Table 2) highlight the geochemical response from known carbonatite and related rock occurrences (Figs. 5-7). Ratios of the maximum concentrations per element show enrichment of soil samples (residual anomaly) in Ba, Mo, and Th, and the <0.18 mm fraction of stream-sediment samples in Yb and Lu relative to carbonatites (primary anomaly; Table 3). In contrast, panned stream-sediment (<2 mm fraction) heavy mineral concentrate (HMC) samples show up to 192 times enrichment of all carbonatite indicator elements, except Sr, relative to carbonatites, soils, and the <0.18 mm fraction of stream-sediment samples. Panned stream-sediment HMC samples enhance the contrast of carbonatite indicators such as Ta (Fig. 6) and thus are the preferred medium for drainage surveys targeting critical metals (Rukhlov et al., 2020a).

Table 1. Provincial lithogeochemical data from carbonatites and carbonate sedimentary rocks.

		Sedimentary carbonate rocks				Carbonatites			
Element	**Unit**	**Count**	**Minimum**	**Maximum**	**Mean**	**Count**	**Minimum**	**Maximum**	**Mean**
SiO_2	wt%	32	0.27	67.44	15.62	600	0.09	35.72	5.33
TiO_2	wt%	34	<0.02	1.42	0.15	594	<0.01	5.96	0.19
Al_2O_3	wt%	34	0.06	10.03	1.97	600	<0.01	12.64	0.68
Fe_2O_3(T)	wt%	35	0.06	9.00	1.37	600	0.51	83.28	8.56
MnO	wt%	35	<0.01	0.35	0.07	599	0.15	4.11	0.69
MgO	wt%	35	0.15	20.80	4.17	600	0.26	26.02	12.63
CaO	wt%	35	7.77	60.60	40.80	600	3.66	54.50	31.44
Na_2O	wt%	35	<0.01	1.82	0.23	600	<0.01	6.84	0.43
K_2O	wt%	35	<0.01	1.65	0.38	600	<0.01	4.79	0.38
P_2O_5	wt%	35	<0.01	0.18	0.07	600	<0.01	14.87	3.15
LOI	wt%	31	9.10	44.30	34.91	598	2.30	43.90	34.92
C(T)	wt%	25	2.03	12.26	9.67	516	0.01	12.90	10.35
S(T)	wt%	27	<0.01	0.48	0.06	515	<0.01	3.97	0.30
F	wt%	1	na	na	0.01	14	<0.01	1.45	0.27
Ag	ppm	22	0.03	0.40	0.09	197	<0.1	5.7	0.54
As	ppm	28	<0.5	17	2.2	192	<0.5	77	3.0
Au	ppb	20	<2	8	1.2	110	<0.5	426	6.7
Ba	ppm	29	<5	2379	275	610	15.1	288595	1825
Be	ppm	15	0.06	1.0	0.67	512	<1	11	0.91
Bi	ppm	16	<0.02	0.2	0.09	192	<0.1	3.1	0.24
Br	ppm	4	<0.5	<1	na	1	na	na	2.8
Cd	ppm	21	<0.2	6.9	0.46	110	<0.1	1.5	0.33
Ce	ppm	28	0.8	51	14.7	611	7.1	53200	1169
Co	ppm	30	<1	50	5.1	586	<1	73	15.5
Cr	ppm	30	3.4	506	38.0	556	<0.1	2230	60.8
Cs	ppm	28	<0.5	2.0	0.48	535	<0.1	114	1.73
Cu	ppm	22	0.4	26	6.1	584	<0.1	308	11.3
Dy	ppm	17	0.28	3.3	1.32	606	0.37	106	11.2
Er	ppm	17	0.15	1.9	0.76	606	0.15	17.8	3.54
Eu	ppm	28	0.04	1.1	0.34	607	0.2	179	10.4
Ga	ppm	17	0.1	8.4	2.91	596	<0.5	126	6.1
Gd	ppm	17	0.36	3.5	1.46	604	0.53	404	25.2
Ge	ppm	2	<0.1	0.4	0.23	81	<1	14	2.1
Hf	ppm	28	0.03	4.4	0.93	584	<0.1	53	1.96
Hg	ppb	15	<10	20	7	110	<10	110	8
Ho	ppm	17	<0.1	0.63	0.260	606	0.06	10.8	1.60
In	ppm	2	<0.02	<0.04	na	81	<0.2	<0.3	na
La	ppm	30	<0.5	24	7.4	611	3.2	40500	734
Lu	ppm	28	0.017	0.3	0.097	607	0.03	2.0	0.326
Mo	ppm	29	0.04	3.0	0.470	478	<0.1	125	3.24
Nb	ppm	27	0.12	22	5.25	609	2.8	6532	576
Nd	ppm	28	1.21	23	7.17	610	3.7	11900	347
Ni	ppm	30	0.98	209	15.9	536	<0.1	1237	38.1
Pb	ppm	23	0.54	19	6.56	586	0.5	643	16.2
Pr	ppm	17	0.23	5.94	2.205	606	0.86	4300	90.0
Rb	ppm	28	0.2	59	12.3	594	<0.1	327	12.7
Sb	ppm	28	<0.1	1.1	0.14	191	<0.1	4.7	0.10
Sc	ppm	27	0.20	26	3.84	207	0.24	62	16.7
Se	ppm	19	0.01	0.5	0.23	110	<0.5	7.3	0.56
Sm	ppm	28	0.23	4.2	1.40	607	0.68	947	42.0
Sn	ppm	17	<0.02	2	0.74	344	<1	25	1.6
Sr	ppm	30	47	3882	914	611	360	>50000	4401
Ta	ppm	28	<0.1	1.4	0.24	599	<0.01	646	101
Tb	ppm	28	0.046	0.64	0.176	607	0.07	36.3	2.77
Th	ppm	30	0.06	7.1	1.64	611	<0.1	>10000	71.6
Tl	ppm	15	0.05	1.3	0.16	197	<0.1	1.3	0.10
Tm	ppm	17	0.02	0.31	0.117	606	0.03	2.17	0.433
U	ppm	28	0.2	2.6	0.79	609	<0.1	379	40.0
V	ppm	23	1	139	26.7	585	<5	2713	49.6
W	ppm	28	0.2	1.4	0.34	350	<0.1	22.5	0.89
Y	ppm	28	1.5	22.3	8.43	611	1.7	323	43.0
Yb	ppm	28	<0.2	1.86	0.636	607	0.19	14.1	2.44
Zn	ppm	29	<1	173	24.4	307	2	1949	77.3
Zr	ppm	28	1	173	38.8	610	<0.1	2978	104.8

Data from Chakhmouradian et al. (2015), Chudy (2013), Dalsin et al. (2015), Gorham (2008), Han et al. (2016), Han and Rukhlov (2020a), Locock (1994), Mäder (1987), Mumford (2009), Rukhlov and Gorham (2007), Simandl et al. (2013), Trofanenko (2014), Trofanenko et al. (2016), and Ya'acoby (2014). **na** - not analyzed.

Table 2. Blue River area lithogeochemical data from rock, soil, RGS stream sediment, and panned stream-sediment heavy mineral concentrate samples.

		Carbonatites					Soil samples					RGS stream sediments					Panned HMC of stream sediments				
Element	Unit	Method	Count	Minimum	Maximum	Mean	Method	Count	Minimum	Maximum	Mean	Method	Count	Minimum	Maximum	Mean	Method	Count	Minimum	Maximum	Mean
TiO_2	wt%	T	477	<0.01	5.96	0.143	na	na	na	na	na	P	208	0.02	1.63	0.252	P	24	0.06	0.43	0.184
Al_2O_3	wt%	T	483	<0.01	12.64	0.374	na	na	na	na	na	P	208	0.77	4.85	2.748	P	24	0.91	4.33	1.721
Fe_2O_3(T)	wt%	T	483	0.51	83.28	8.743	na	na	na	na	na	T	208	2.29	12.53	6.440	T	8	6.86	18.42	12.603
MnO	wt%	T	483	0.15	1.53	0.692	na	na	na	na	na	P	208	<0.01	0.16	0.044	P	24	0.03	0.30	0.106
MgO	wt%	T	483	0.49	26.02	13.204	na	na	na	na	na	P	208	0.22	3.56	1.188	P	24	0.36	1.41	0.694
CaO	wt%	T	483	3.66	52.87	31.759	na	na	na	na	na	P	208	0.11	6.28	0.807	P	24	0.14	4.18	0.733
Na_2O	wt%	T	483	<0.01	3.63	0.364	na	na	na	na	na	T	208	0.62	3.10	1.972	T	8	0.67	2.70	1.923
K_2O	wt%	T	483	<0.01	4.79	0.176	na	na	na	na	na	P	208	<0.01	1.76	0.640	P	24	0.08	0.70	0.274
P_2O_5	wt%	T	483	0.01	14.87	3.287	na	na	na	na	na	P	208	0.09	2.27	0.310	P	24	0.08	2.34	0.318
S(T)	wt%	T	483	<0.01	2.38	0.293	na	na	na	na	na	P	208	<0.01	1.56	0.091	P	24	<0.01	0.08	0.017
Ag	ppb	P	97	<100	600	124	P	8082	<100	3100	108	P	208	6	631	47	P	626	<2	3400	80
As	ppm	P	97	<0.5	5.3	0.93	P	8082	<0.5	4932	1.5	T, P	208	<0.1	7.8	0.93	P	626	<0.1	2511	26
Au	ppb	P	97	<0.5	426	7.4	P	7976	<0.5	834	1.2	P	208	<0.2	34	1.3	P	607	<0.2	4703	42
Ba	ppm	T	483	15	5823	218	T	8428	<1	8267	588	T	208	85	1300	503	T	610	4	21601	172
Be	ppm	T	418	<1	11	0.62	T	8165	<1	32	2.0	P	na	na	na	na	T	586	<1	37	1.2
Bi	ppm	P	97	<0.1	1.1	0.10	P	8082	<0.1	51	0.26	P	208	0.04	1.8	0.33	P	626	<0.1	578	8.0
Cd	ppm	P	97	<0.1	1.5	0.34	P	8082	<0.1	84	0.14	P	208	0.01	0.51	0.08	P	626	<0.1	5479	31
Ce	ppm	T	483	7.1	2418	318	T	8428	<0.1	1477	100	T	208	62	1010	260	T	615	70	28419	2737
Co	ppm	T	483	0.6	73	16	T	8428	<0.2	272	12	T	208	<5	116	18	T	615	3.9	492	29
Cr	ppm	T	464	<0.1	2230	66.5	na	na	na	na	na	T	208	28	370	109	T	8	123	411	215
Cs	ppm	T	432	<0.1	48	1.5	T	8428	<0.1	23	4.5	T	208	<1	12	4.2	T	615	<0.1	5.1	0.65
Cu	ppm	P	481	0.2	308	9.8	P	8082	1.9	355	20	P	208	3	166	34	P	626	1.2	1195	28
Dy	ppm	T	483	0.37	27	9.2	T	8428	<0.05	33	4.8	na	na	na	na	na	T	615	3.6	1224	119
Er	ppm	T	483	0.15	14	3.2	T	8428	<0.03	13	2.7	na	na	na	na	na	T	615	2.5	687	67
Eu	ppm	T	483	0.2	22	6.3	T	8428	<0.02	24	1.4	T	180	0.9	8.4	3.13	T	615	1.2	207	20
Ga	ppm	T	483	<0.5	28	2.9	T	8428	<0.5	34	17	P	208	1.6	11	5.3	T	615	2.8	83	16
Gd	ppm	T	483	0.53	52	17	T	8428	<0.05	52	5.6	na	na	na	na	na	T	615	0.2	1430	149
Hf	ppm	T	481	<0.1	53	1.5	T	8428	<0.1	49	6.3	T	208	4.0	87	15	T	615	3.4	670	42
Hg	ppb	P	97	<10	110	7.1	P	7976	<10	380	41	P	208	<5	73	14	P	610	<5	160	7.6
Ho	ppm	T	483	0.06	4.9	1.4	T	8428	<0.02	5.5	0.94	na	na	na	na	na	T	615	0.77	844	32
La	ppm	T	483	3.2	1695	149	T	8428	<0.1	1269	51	T	208	28	509	139	T	615	32	13647	1353
Lu	ppm	T	483	0.03	2.0	0.30	T	8428	<0.01	1.5	0.40	T	208	<0.2	3.9	1.09	T	615	0.33	96	11
Mo	ppm	P	376	<0.1	21	0.46	P	8082	<1	85	2.3	P	208	0.11	3.8	0.99	P	626	0.2	738	9.8
Nb	ppm	T	483	5	6532	610	T	8428	<0.1	5507	35	na	na	na	na	na	T	615	11.2	16890	562
Nd	ppm	T	483	3.7	618	141	T	8428	<0.3	483	41	T	180	27	420	102	T	615	19	>10000	1098
Ni	ppm	T, P	436	<0.1	1237	43	P	8082	1.2	1025	18	P	208	2.7	137	26	P	626	2.0	2654	46
Pb	ppm	P	483	<1	30	5.4	P	8082	1.8	547	8.9	P	208	1.93	15	5.8	P	626	0.9	934	18
Pr	ppm	T	483	0.86	210	36	T	8428	<0.02	124	11	na	na	na	na	na	T	615	8.2	2813	296
Rb	ppm	T	475	<0.1	249	5.3	T	8428	<0.1	274	83	T	208	28	220	93	T	615	1.3	94	14
Sb	ppm	P	97	<0.1	0.2	0.056	P	8082	<0.1	42	0.075	P	208	<0.02	0.2	0.029	P	626	<0.1	7442	57
Sc	ppm	T	120	1.0	34	10	na	na	na	na	na	T	208	6.4	35	17	T	8	19	46	31
Se	ppm	P	97	<0.5	1.9	0.47	P	7976	<0.5	12.6	0.19	P	208	0.1	2.2	0.57	P	597	<0.5	35.7	1.11
Sm	ppm	T	483	0.68	78	22	T	8428	<0.05	76	6.8	T	208	5	74	21	T	615	<1	1576	172
Sn	ppm	T	244	<1	25	1.2	T	8428	<1	35	2.6	na	na	na	na	na	T	615	<1	125	8.6
Sr	ppm	T	483	366	10559	4179	T	8428	<0.5	4201	203	P	208	5.5	186	30	T	615	3.1	4528	144
Ta	ppm	T	483	1.1	646	123	T	8428	<0.1	405	2.2	T	208	<1	13	2.8	T	615	1.2	2475	43
Tb	ppm	T	483	0.07	6.5	2.1	T	8428	<0.01	6.7	0.89	T	208	0.60	9.2	2.8	T	615	0.68	213	22
Th	ppm	T	483	<0.1	174	6.7	T	8428	<0.2	484	15	T	208	8.9	162	41	T	615	7.4	4080	459
Tl	ppm	P	97	<0.1	0.3	0.060	P	8120	<0.1	14	0.18	P	208	<0.02	0.72	0.26	P	626	<0.1	2.9	0.029
Tm	ppm	T	483	0.03	2.1	0.41	T	8428	<0.01	1.6	0.42	na	na	na	na	na	T	615	0.35	104	11
U	ppm	T	483	<0.1	347	44	T	8428	<0.1	197	3.9	T	208	2.2	33	11	T	615	1.7	2136	107
V	ppm	T	482	<5	2713	44	T	8428	<8	499	88	P	208	6	74	35	T	615	43	3603	310
W	ppm	T	250	<0.1	7.7	0.91	T	8428	<0.5	176	2.0	T	207	<1	9	2.3	T	615	1.1	3215	53
Y	ppm	T	483	1.7	135	38	T	8428	<0.1	148	27	na	na	na	na	na	T	615	23	6438	683
Yb	ppm	T	483	0.19	13	2.3	T	8428	<0.05	10	2.7	T	208	<2	26	7.3	T	615	2.3	636	71
Zn	ppm	P	204	2	288	35	P	8082	5	935	43	P	208	16	201	53	P	626	5	163	27
Zr	ppm	T	483	<0.1	2978	86	T	8428	9.5	1978	220	T	28	<200	2300	621	T	615	113	41442	1707

Data from Chudy (2013), Dahrouge and Reeder (2001), Dahrouge and Wolbaum (2004), Gorham (2008), Gorham et al. (2009, 2011a, 2011b), Han and Rukhlov (2017, 2020b), Reeder and Dahrouge (2002), Rukhlov and Gorham (2007), Smith and Dahrouge (2003). Method abbreviations: **T** – total determination via instrumental neutron activation analysis (INAA; RGS stream sediment samples only) or lithium-borate fusion with a combination of inductively coupled plasma atomic emission spectroscopy (ICP-AES) and inductively coupled plasma mass spectrometry (ICP-MS). **P** – partial digestion using modified aqua regia and a combination of ICP-AES and ICP-MS. **na** - not analyzed.

Table 3. Blue River area relative enrichment of selected carbonatite indicator elements in different sample media.

Element	S/P	Db/P	Db/S	Dc/P	Dc/S	Dc/Db
Sr	0.4	0.02	0.04	0.4	1.1	24
Ba	1.4	0.2	0.2	3.7	2.6	17
Mo	4.0	0.2	0.05	35	8.7	192
Nb	0.8	na	na	2.6	3.1	na
Ta	0.6	0.02	0.03	3.8	6.1	190
La	0.7	0.3	0.4	8.1	11	27
Ce	0.6	0.4	0.7	11.8	19	28
Eu	1.1	0.4	0.4	9.2	8.7	25
Yb	0.8	2.0	2.6	48	63	24
Lu	0.8	2.0	2.5	48	62	24
Y	1.1	na	na	48	43	na
Th	2.8	0.9	0.3	23	8.4	25
U	0.6	0.1	0.2	6.2	11	65

Enrichment factors calculated as ratios of maximum element concentrations in different sample media (Table 2). **Db** – the <0.18 mm sieved fraction of bulk stream sediment (RGS sample medium), **Dc** – panned heavy mineral concentrate (HMC) of the <2 mm sieved fraction of stream sediment, **P** – rock (carbonatite), and **S** – soil. Values >1 indicate enrichment of the numerator medium relative to the denominator and vice versa. **na** - not analyzed.

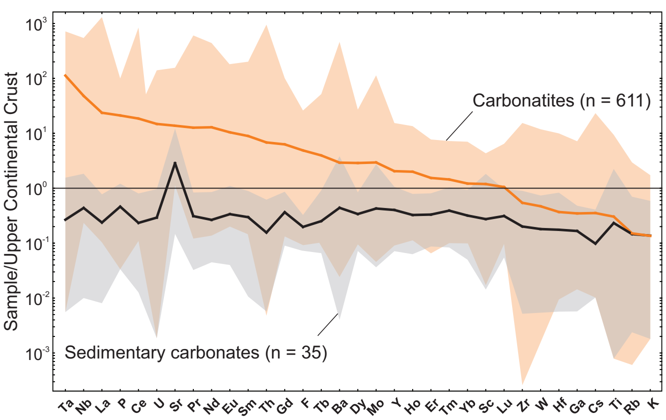

Fig. 4. Compositional ranges and mean compositions (solid lines) of carbonatites and sedimentary carbonate rocks in British Columbia, normalized to the upper continental crust of Rudnick and Gao (2005). Data from Mäder (1987), Locock (1994), Rukhlov and Gorham (2007), Gorham (2008), Mumford (2009), Chudy (2013), Simandl et al. (2013), Trofanenko (2014), Ya'acoby (2014), Chakhmouradian et al. (2015), Dalsin et al. (2015), Han et al. (2016), Trofanenko et al. (2016), and Han and Rukhlov (2020a).

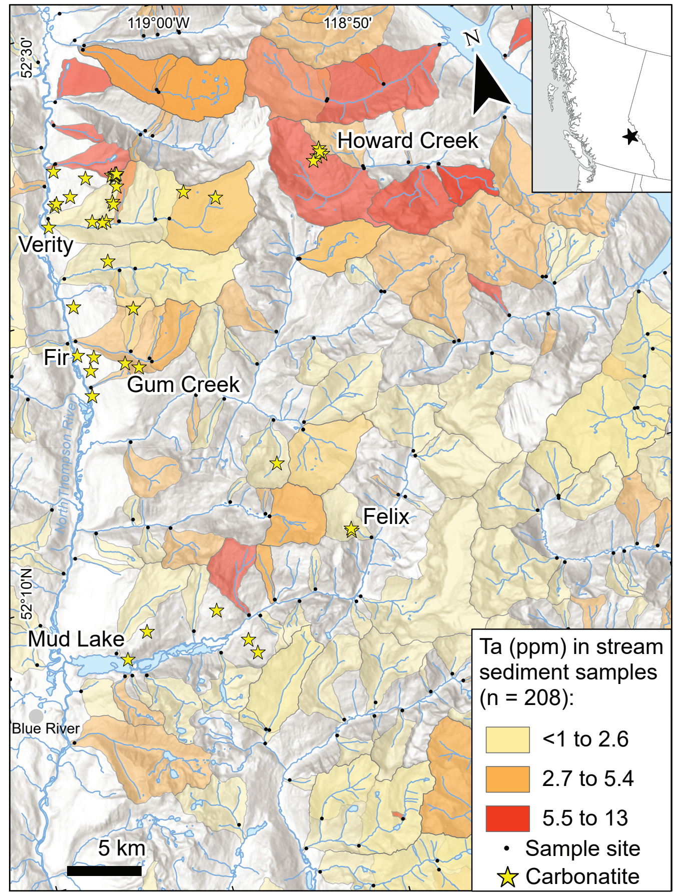

Fig. 5. Blue River area, tantalum-themed catchment basins of regional geochemical survey stream-sediment samples (<0.18 mm fraction; after Han and Rukhlov, 2017, 2020a). Carbonatite occurrences after Rukhlov and Gorham (2007), Gorham (2008), Gorham et al., 2009, 2011a, 2011b, 2013), Millonig and Groat (2013), and Rukhlov et al. (2018).

5. Regional geochemical survey data

Collected as part of the Regional Geochemical Survey (RGS) program since 1976, the data for this study (Table 4) include the multi-element determinations for a total of 11502 stream-sediment (<0.18 mm fraction) and water samples at an average sampling density of about 1 site per 10 km^2 (Han and Rukhlov, 2017; 2020b; Lett and Rukhlov, 2017). Considering the emplacement ages of carbonatites and related rocks (>320 Ma), the selected stream sediment samples have catchment basins (Cui et al., 2009) that are underlain by the >320 Ma rocks in the study area (Fig. 2). The determinations by aqua-regia digestion with atomic absorption spectrometry (AAS) or a combination of inductively coupled plasma atomic emission spectroscopy (ICP-AES) and inductively coupled plasma mass spectrometry (ICP-MS) are underestimated for elements hosted by silicate and oxide minerals because of only partial dissolution in HCl-HNO_3 acid mixtures. In contrast, instrumental neutron activation analysis (INAA) provides total determinations. Elevated concentrations of carbonatite indicator elements such as La (Fig. 8), Ta (Fig. 9), U (Fig. 10), and P (Fig. 11) in the stream sediments reflect local background variations, including at known carbonatite and related rock occurrences.

6. Discriminant analysis method

Below we evaluate the multi-element drainage geochemical data to identify the carbonatite signature (Fig. 12). To construct

Table 4. Regional geochemical survey (RGS) lithogeochemical data from stream-sediment samples.

Variable	Method	Unit	Count	<MDL[1]	Mean	Minimum	Median	Percentiles			Maximum	Skewness	DPA[2]
								87th	93rd	98th			
Area[3]		km^2	11502		9.9	0.008	5.5	18	28	54	193	4	
Ag	AAS, ICP-MS	ppb	11073	0.13	122	<2	57	184	278	587	>100000	87	
Al	ICP-AES	wt%	11002	0.00	1.2	0.02	1.07	1.75	2.03	2.53	5.86	1	
As	AAS, ICP-MS	ppm	11467	0.68	9.2	<0.1	4.5	14	21	42	5370	68	
Au	ICP-MS	ppb	11263	11	14	<0.2	1.2	7.6	13	47	40630.4	78	
Ba	ICP-MS	ppm	11002	0.00	136	2.2	72	230	361	856	2769	5	
Ba	INAA	ppm	10104	0.48	835	<50	603	1200	1500	3400	37000	11	Y
Bi	AAS, ICP-MS	ppm	11117	0.97	0.29	<0.02	0.19	0.40	0.51	1.0	125	61	
Ca	ICP-AES	wt%	11002	0.01	2.5	<0.02	0.62	5.87	10.22	18.79	40.00	3	Y
Cd	AAS, ICP-MS	ppm	11298	2.0	0.53	<0.01	0.13	0.5	0.93	3	644.53	83	
Ce	INAA	ppm	10107	0.33	129	<3	100	210	270	430	1450	4	Y
Co	ICP-MS	ppm	11002	0.00	12	0.3	11	18	22	31	173	5	
Co	INAA	ppm	10107	5.4	15	<1	14	24	29	41	217	4	
Cr	ICP-MS	ppm	11002	0.00	27	0.7	21	43	55	90	1051	12	
Cr	INAA	ppm	10107	0.63	115	<5	81	170	230	390	8750	19	
Cs	INAA	ppm	10106	2.6	3.8	<0.5	3.1	6.0	7.6	12	67	5	
Cu	AAS, ICP-MS	ppm	11497	0.00	27	0.71	22	44	54	81	1200	14	
Eu	INAA	ppm	1851	5.0	2.0	<0.2	1.8	3.2	4.0	5.7	20	3	
F	ISE	ppm	4259	0.00	485	50	430	750	890	1189	2040	1	
Fe	ICP-AES	wt%	11002	0.00	2.4	0.04	2.25	3.51	3.95	4.75	26.0	2	Y
Fe	INAA	wt%	10107	0.12	3.6	<0.2	3.5	5.1	5.8	7.3	26.3	1	
Ga	ICP-MS	ppm	11002	0.08	3.5	<0.2	3.3	5.4	6.3	8.2	17	1	
Hf	INAA	ppm	10107	2.3	9.5	<1	8	15	20	31	308	8	
Hg	AAS, ICP-MS	ppb	11000	5.8	40	<5	26	66	92	166	4480	29	
K	ICP-AES	wt%	11002	0.32	0.13	<0.01	0.07	0.25	0.36	0.64	1.46	3	Y
La	ICP-MS	ppm	11002	0.06	20	<0.5	16	29	37	62	1146	19	
La	INAA	ppm	10107	0.48	71	<2	55	119	150	242	1160	5	Y
Li	ICP-MS	ppm	5743	0.00	21	0.5	18	38	46	60	131	1	
Lu	INAA	ppm	10107	28	0.48	<0.05	0.40	0.87	1.1	1.7	21	9	
Mg	ICP-AES	wt%	11002	0.00	0.96	0.03	0.64	1.48	2.18	4.96	21.79	5	Y
Mn	AAS, ICP-AES	ppm	11497	0.00	522	15	402	770	984	1765	>30000	21	Y
Mo	ICP-MS	ppm	11002	0.00	1.1	0.02	0.53	1.6	2.7	6.6	113	17	Y
Na	ICP-AES	wt%	11002	5.4	0.012	<0.001	0.006	0.022	0.032	0.06	1.76	30	
Na	INAA	wt%	10102	1.2	1.1	<0.1	1.0	1.9	2.2	2.7	10.3	1	
Nb	ICP-MS	ppm	5743	3.5	0.51	<0.02	0.27	1.1	1.4	2.3	8.3	4	
Nd	INAA	ppm	1462	0.21	70	<5	59	120	140	207	638	3	
Ni	ICP-MS	ppm	11002	0.00	33	0.3	25	49	62	112	2369	22	Y
P	ICP-AES	wt%	11002	0.00	0.09	0.007	0.074	0.129	0.157	0.234	1.064	8	Y
Pb	AAS, ICP-MS	ppm	11497	0.00	17	0.57	10	21	27	47	>20000	98	Y
Rb	INAA	ppm	10107	0.86	87	<5	84	121	140	170	400	1	
S	ICP-AES	wt%	11002	20	0.059	<0.01	0.03	0.10	0.14	0.31	6.77	21	
Sb	ICP-MS	ppm	11002	3.3	0.39	<0.02	0.15	0.58	0.98	2.3	297	81	
Sb	INAA	ppm	10106	25	0.88	<0.1	0.4	1.4	2.2	4.9	566	82	
Sc	ICP-MS	ppm	11002	0.00	2.6	0.1	2.3	4.0	5.0	7.4	20	2	
Sc	INAA	ppm	10107	0.04	12	<0.5	11	17	20	26	107	2	Y
Se	ICP-MS	ppm	11002	7.0	0.70	<0.1	0.4	1.2	1.7	3.2	58	19	
Sm	INAA	ppm	10107	0.19	10	<0.1	8.2	16	21	34	165	5	Y
Sr	ICP-MS	ppm	11002	0.00	66	0.3	31	127	199	357	1978	7	Y
Ta	INAA	ppm	10107	13	1.7	<0.5	1.5	2.8	3.4	5.7	70	12	
Tb	INAA	ppm	10107	14	1.3	<0.5	1.1	2.1	2.7	4.2	25	6	
Te	ICP-MS	ppm	11002	59	0.02	<0.01	<0.01	0.04	0.05	0.09	10	92	
Th	ICP-MS	ppm	11002	0.16	5.4	<0.1	4.4	9.5	12	16	363	28	
Th	INAA	ppm	10107	0.12	19	<0.2	14	30	41	75	488	7	Y
Ti	ICP-AES	wt%	11002	0.63	0.051	<0.001	0.029	0.112	0.144	0.216	0.990	4	Y
Tl	ICP-MS	ppm	11002	9.7	0.12	<0.02	0.08	0.23	0.31	0.46	3.3	7	
U	ICP-MS	ppm	11002	0.06	2.7	<0.1	1.3	4.1	6.8	15	244	18	
U	INAA	ppm	10105	0.25	6.7	<0.2	4.7	11	15	26	228	10	Y
V	AAS, ICP-MS	ppm	11199	0.32	30	<1	24	53	67	97	500	3	Y
W	ICP-MS	ppm	11002	58	0.49	<0.05	<0.05	0.5	1.2	4.3	101	22	
W	INAA	ppm	10106	78	1.7	<1	<1	3	4	9	1950	92	
Y	ICP-MS	ppm	5743	0.00	9.6	0.27	7.4	13	17	31	647	23	
Yb	INAA	ppm	10107	32	2.8	<0.2	3.0	5.0	6.3	9.5	59	3	
Zn	AAS, ICP-MS	ppm	11497	0.00	99	2.8	59	102	140	360	88000	89	Y
Zr	ICP-MS	ppm	5743	1.9	1.6	<0.1	1.2	2.9	3.7	5.7	103	25	
Zr	INAA	ppm	7035	28	394	<200	330	640	830	1400	15000	10	

[1] Percentage of values less than the minimum detection limit (MDL).
[2] Variables having value of 'Y' (shaded rows) used in discriminant projection analysis (DPA).
[3] Area of catchment basin in square kilometres.
Analytical method abbreviations: **AAS** – aqua regia digestion and atomic absorption spectrometry, **ICP-AES** – aqua regia digestion and inductively coupled plasma atomic emission spectroscopy, **ICP-MS** – aqua regia digestion and inductively coupled plasma mass spectrometry, **INAA** – instrumental neutron activation analysis, **ISE** – Na_2CO_3+KNO_3 fusion followed by H_2O leach and ion selective electrode. Data from Han and Rukhlov (2017; 2020b).

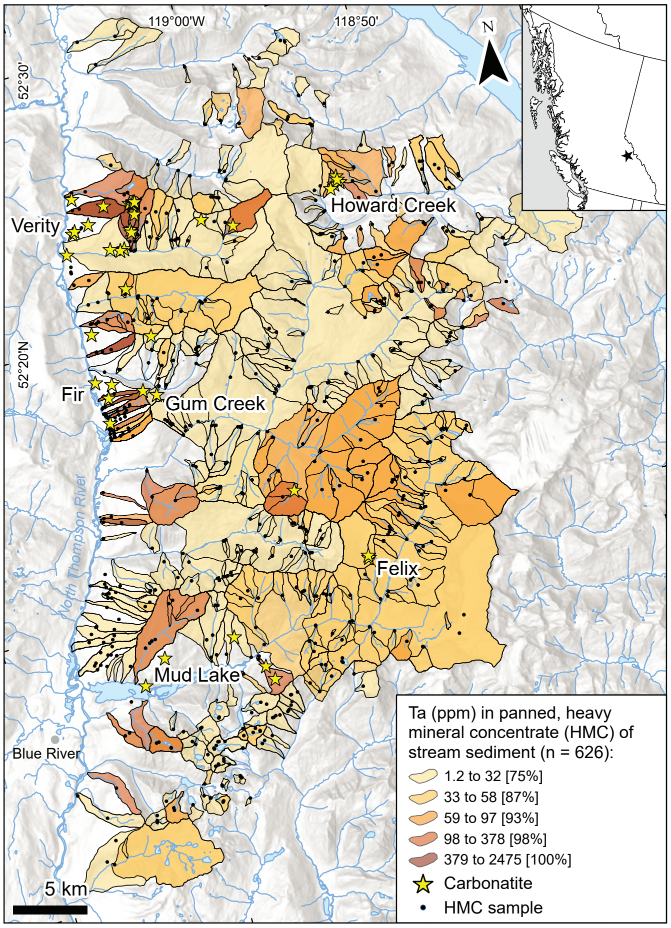

Fig. 6. Blue River area, tantalum-themed, percentile-ranked catchment basins of panned, stream-sediment (<2 mm fraction), heavy mineral concentrate (HMC) samples. Data and carbonatite occurrences from Dahrouge and Reeder (2001), Reeder and Dahrouge (2002), Smith and Dahrouge (2003), Dahrouge and Wolbaum (2004), Rukhlov and Gorham (2007), Gorham (2008), Gorham et al. (2009, 2011a, 2011b, 2013).

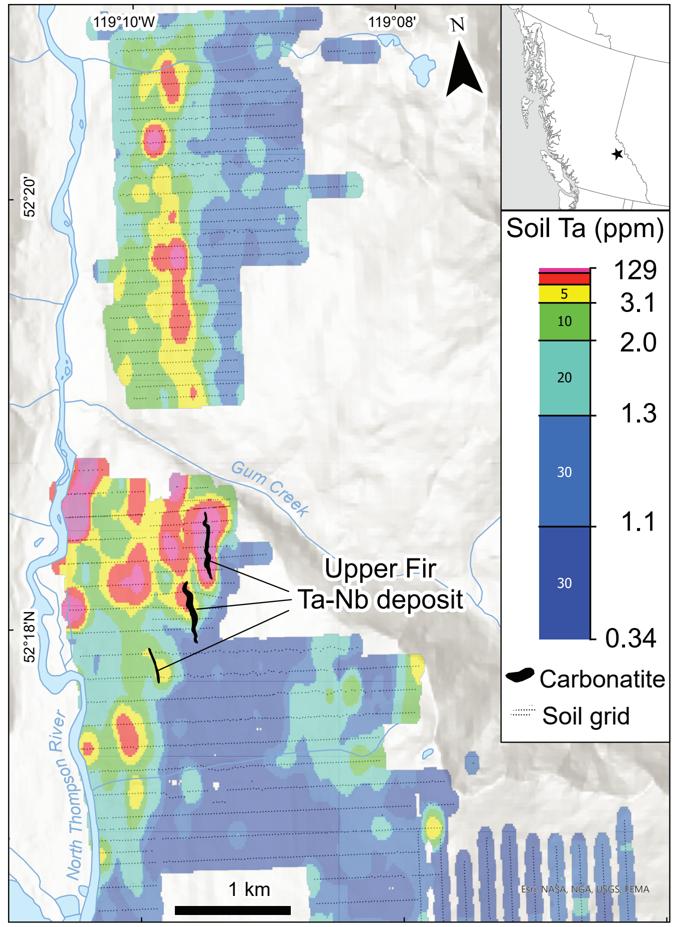

Fig. 7. Blue River area, percentile-gridded, Ta concentrations (ppm) in soil samples (after Reeder and Dahrouge, 2002; Smith and Dahrouge, 2003; Dahrouge and Wolbaum, 2004; Rukhlov and Gorham, 2007; Gorham, 2008; Gorham et al., 2009, 2011a, 2011b). Upper Fir carbonatite-hosted Ta-Nb deposit footprint after Kraft (2011) and Gorham et al. (2013).

the best criteria for discriminating between carbonatite and other signals using multi-element stream-sediment data, we performed a discriminant projection analysis (DPA) on a sub-set of stream-sediment data taken from the regional geochemical survey area (Fig. 13) in ioGAS™ software. DPA is a supervised multivariate statistical technique that determines an optimum projection of multivariate data into a lower dimensional (e.g., bivariate) space to achieve the best separation between user-defined groups (Flury, 1997). The DPA uses an a priori knowledge of the group memberships to define discriminant parameters (DP1, DP2, DPn) that maximize the ratio of the within-groups sum of squares (W) to between-groups sum of squares (B) matrices (W/B). The between-groups matrix is effectively the covariance of the group means and the within-groups matrix is the weighted covariance matrix for the groups. Our group 1 includes stream-sediment data that are downstream of known carbonatite or related rock occurrences (n=53); group 2 consists of stream sediments derived mainly from carbonate sedimentary rocks (n=90); and group 3 is a random 20% sub-sample of all stream-sediment data in the study area (n=1943; Fig. 13). A ranked element contrast (REC) plot for the average Group 1 stream sediment relative to the median stream sediment in the study area (Fig. 14a) reveals maximum contrast of the carbonatite and related-rock association (Th-K-REE-W-U-Ti-Ta-Hf-Mo-P-Sr). In contrast, the average of a random sub-set of stream sediment samples (Group 3) shows maximum contrast of precious and base metals, along with other pathfinders of hydrothermal ore deposits (Fig. 14b); the ranked element contrast profile for group 2 is similar to that of group 3. Based on the ranked element contrast associations, we selected 20 elements that have <1% of values below the minimum detection limit for the discriminant projection analysis (Table 4). We performed the discriminant projection analysis on a random 50% training sub-set of the group 1 to 3 data (Fig. 12). The constructed discriminant parameters (DP1 and DP2) are linear combinations of the log10-transformed element concentrations that optimally separate the data of groups 1 to 3 (Table 5) as summarized in Equations 1 and 2.

$$DP1 = 0.5125 \cdot Ba - 0.1132 \cdot Ca + 0.019 \cdot K - 0.3508 \cdot Mg - 0.7108 \cdot Mn - 0.7341 \cdot Mo - 0.8466 \cdot Ni - 0.8647 \cdot P + 0.8483 \cdot Pb + 1.108 \cdot Sc - 0.8055 \cdot Sm - 0.1415 \cdot Sr - 2.78 \cdot Th - 0.1456 \cdot Ti + 0.2234 \cdot U - 0.2579 \cdot V + 0.9749 \cdot Zn - 2.181 \cdot La + 2.225 \cdot Fe + 1.957 \cdot Ce + 0.038113$$ (Eqn. 1)

$$DP2 = 1.008 \cdot Ba - 0.6432 \cdot Ca - 0.834 \cdot K + 2.034 \cdot Mg - 0.1111 \cdot Mn - 0.2682 \cdot Mo - 0.5129 \cdot Ni - 0.2222 \cdot P + 0.3704 \cdot Pb + 0.01757 \cdot Sc - 0.02553 \cdot Sm - 0.7922 \cdot Sr - 1.464 \cdot Th + 1.035 \cdot Ti + 2.46 \cdot U - 0.8935 \cdot V + 0.2481 \cdot Zn + 0.2286 \cdot La + 0.5293 \cdot Fe - 0.7624 \cdot Ce + 1.6581$$ (Eqn. 2)

Calculated contours of constant Mahalanobis distance at $\chi^2 = 0.975$, using robust multivariate estimation (Campbell, 1980), outline most of the data in each group (Fig. 15a). Projecting a random 50% test sub-set of the group 1 to 3 data, which were not used in the discriminant projection analysis, into the DP1 versus DP2 space validates separation of most of the data in each group (Fig. 15c). The DP1 contributes 73% in discriminating the stream-sediment data downstream of known carbonatites and other stream-sediment data, with the calculated Pearson correlation coefficients of the DP1 variables showing significant contributions of Th, La, Sm, Ce, U, K, P, and Ti (Table 5).

We then used the training sub-set of the group 1 to 3 data to construct the DP1 versus DP2 discrimination diagram with a boundary separating most of the data from stream sediments downstream of known carbonatite or related-rock occurrences and other stream-sediment data (combined groups 2 and 3) using the Auto-Domain Classification Diagram tool in ioGAS™, based on the lowest Mahalanobis distance (Fig. 15b). The final discrimination diagram DP1 versus DP2 with the statistically defined boundary separating carbonatite or related rock sources and other rock sources is validated by the test sub-set of the stream-sediment data (Fig. 15d).

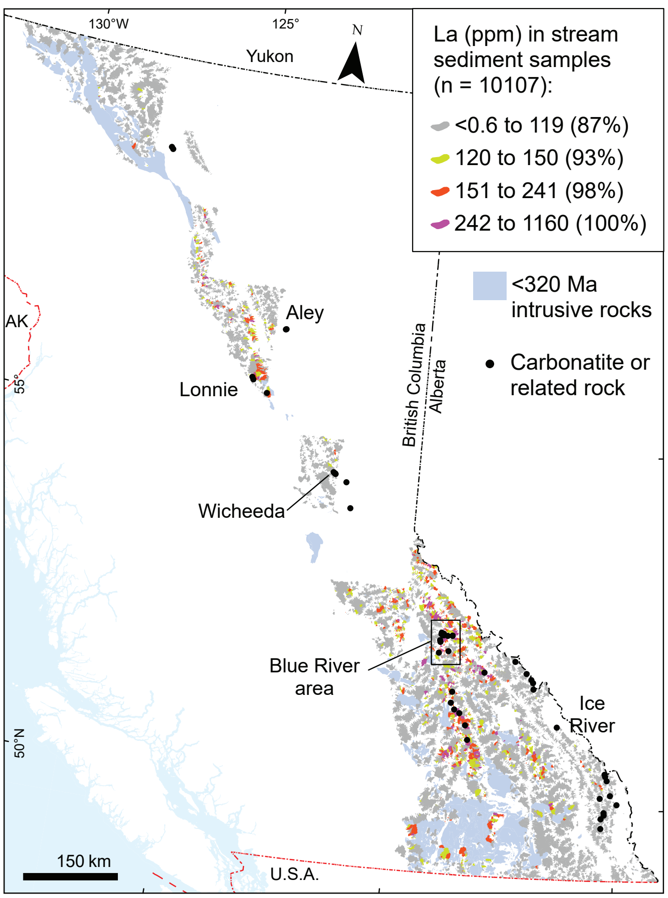

Fig. 8. Regional geochemical survey area, lanthanum-themed, percentile-ranked catchment basins of stream-sediment samples (<0.18 mm fraction; after Han and Rukhlov, 2017, 2020b). Carbonatite and related-rock occurrences after Höy (1988), Parrish and Scammell (1988), Pell (1994), Millonig and Groat (2013), and Rukhlov et al. (2018). The post-320 Ma intrusive rocks from BC Digital Geology version 2021-12-19 (Cui et al., 2017).

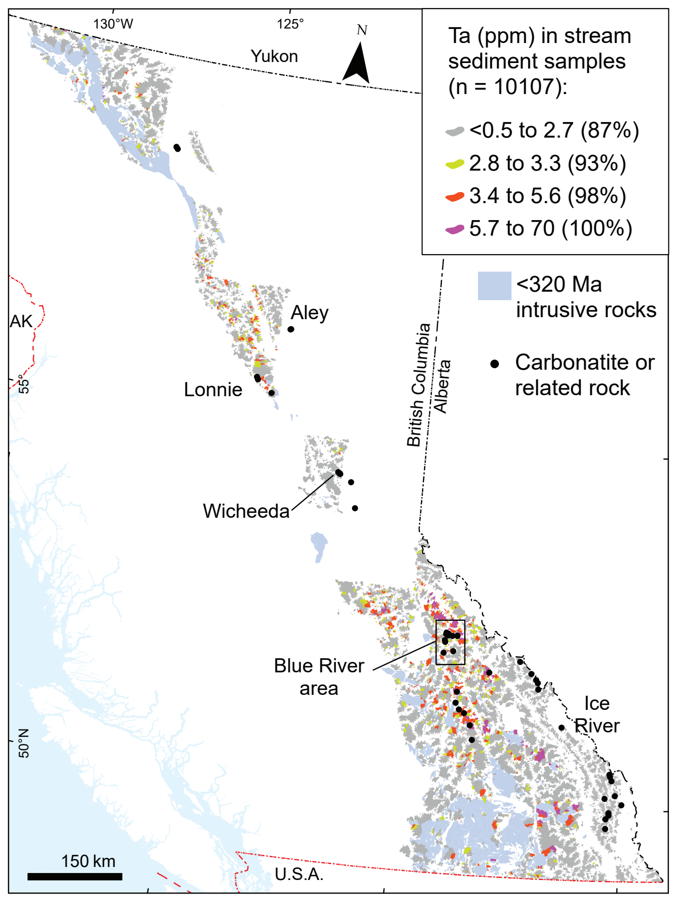

Fig. 9. Regional geochemical survey area, tantalum-themed, percentile-ranked catchment basins of stream-sediment samples (<0.18 mm fraction; after Han and Rukhlov, 2017, 2020b). Carbonatite and related-rock occurrences after Höy (1988), Parrish and Scammell (1988), Pell (1994), Millonig and Groat (2013), and Rukhlov et al. (2018). The post-320 Ma intrusive rocks from BC Digital Geology version 2021-12-19 (Cui et al., 2017).

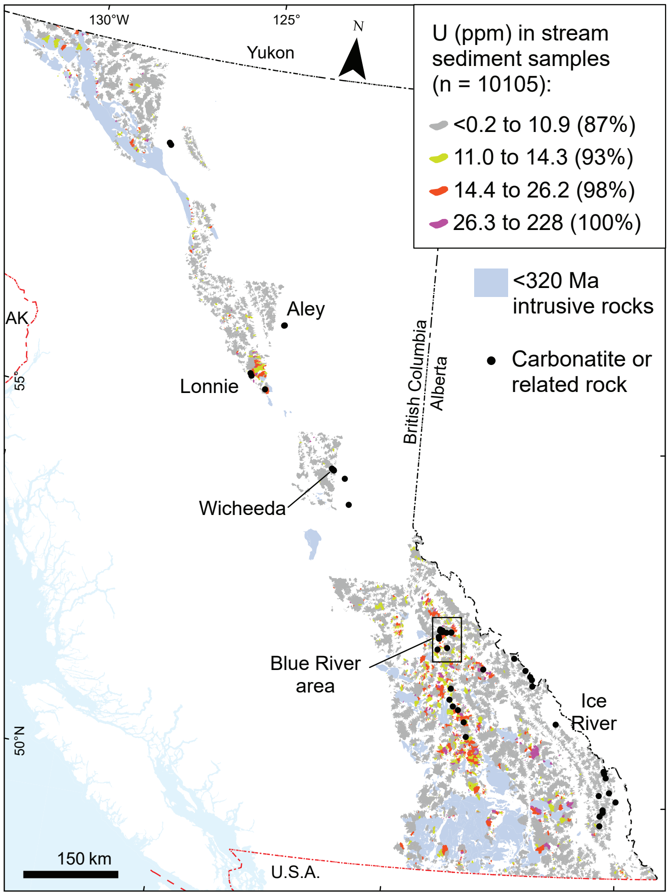

Fig. 10. Regional geochemical survey area, uranium-themed, percentile-ranked catchment basins of stream-sediment samples (<0.18 mm fraction; after Han and Rukhlov, 2017, 2020b). Carbonatite and related-rock occurrences after Höy (1988), Parrish and Scammell (1988), Pell (1994), Millonig and Groat (2013), and Rukhlov et al. (2018). The post-320 Ma intrusive rocks from BC Digital Geology version 2021-12-19 (Cui et al., 2017).

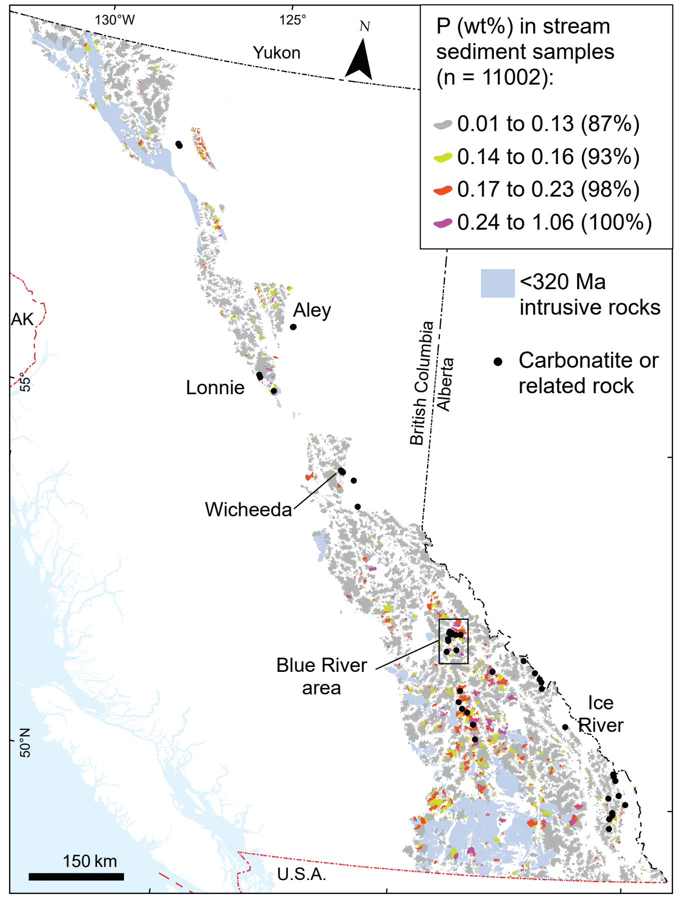

Fig. 11. Regional geochemical survey area, phosphorous-themed, percentile-ranked catchment basins of stream-sediment samples (<0.18 mm fraction; after Han and Rukhlov, 2017, 2020b). Carbonatite and related-rock occurrences after Höy (1988), Parrish and Scammell (1988), Pell (1994), Millonig and Groat (2013), and Rukhlov et al. (2018). The post-320 Ma intrusive rocks from BC Digital Geology version 2021-12-19 (Cui et al., 2017).

7. Discriminant analysis results

7.1. A 'carbonatite index'

Applied to all the regional geochemical survey stream-sediment data in the study area, the DP1 versus DP2 discrimination diagram identified a total of 721 stream sediment samples (6.3% of all the data) showing a multivariate carbonatite or related rock signal (Fig. 16). Herein we refer to this signal, which is recast as the DP1 value multiplied by minus one, as the 'carbonatite index'. The percentile-ranked index highlights prospective stream basins for carbonatite- and related rock-hosted critical metals (Fig. 17). Stream-sediment data showing carbonatite index scores greater than the 93rd percentile (n=50) reveal elevated concentrations of carbonatite indicator elements such as REE, Nb, Ta, Ti, Zr, Hf, Th, U, P, K, and Na, along with indicators of other mineralization-types (e.g., granitoid-related rare metals, precious and base metals), relative to the median (background) concentrations in stream sediments of the study area (Table 6). These geochemical anomalies conspicuously follow a trend of known carbonatite occurrences in the Blue River and Frenchman Cap areas, extending it both to the northwest and southeast (Fig. 18).

7.2. Measure of geochemical anomaly

The quantity of metal above background (or predicted geochemical resources) based on productivity of an element in a dispersion stream is a parametric and thus an objective measure of a geochemical anomaly, which is the basis of evaluating prospective areas (Rukhlov et al., 2020a, b). The productivity of an element in an ideal dispersion stream, P_x (in m^2%) is given in Equation 3.

$$P_x = (1/k) \cdot S_x \cdot (C_x - C_b) \qquad \text{(Eqn. 3)}$$

where

$k <> 1$ is the local proportionality coefficient between the productivity of an element in the dispersion stream and productivity of an element in the secondary or residual dispersion halo (soil anomaly), which depends on hydrography and individual properties of elements resulting in their supergene enrichment or leaching.

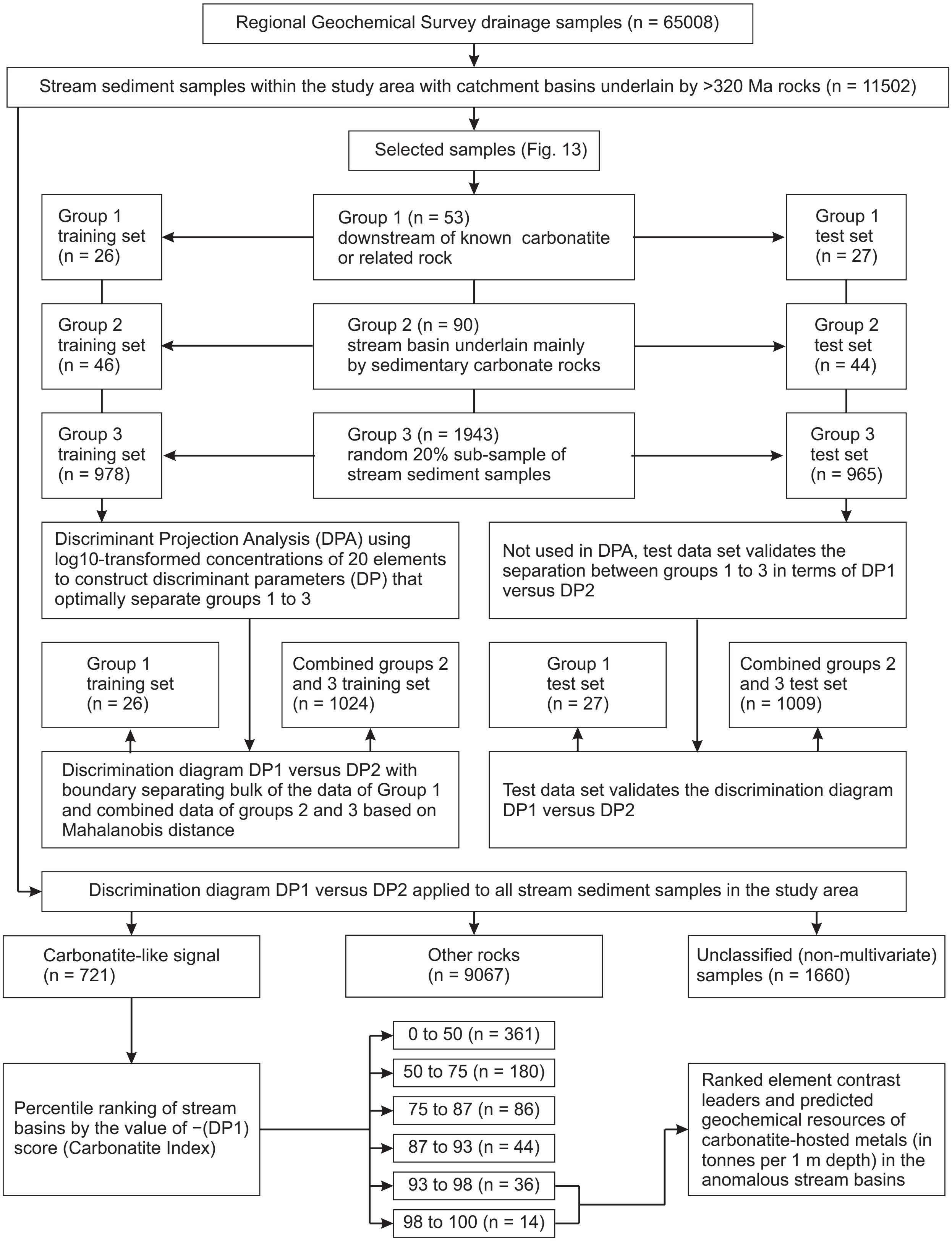

Fig. 12. Workflow used in this study.

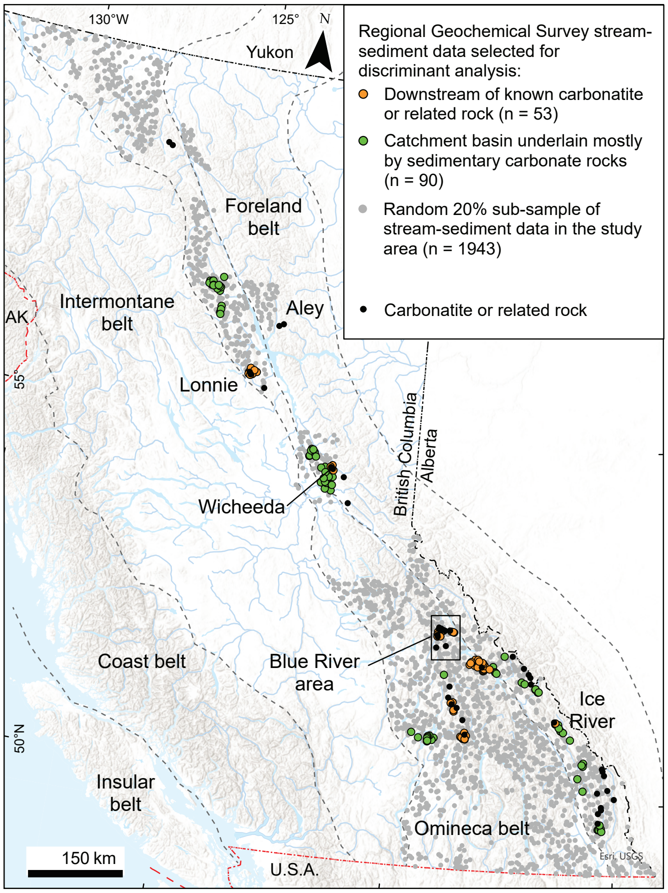

Fig. 13. Selected stream-sediment data from regional geochemical survey area used in training and validating discriminant analysis (after Han and Rukhlov, 2017, 2020b). Carbonatite and related-rock occurrences after Höy (1988), Parrish and Scammell (1988), Pell (1994), Millonig and Groat (2013), and Rukhlov et al. (2018). Morphotectonic boundaries after Gabrielse et al. (1991).

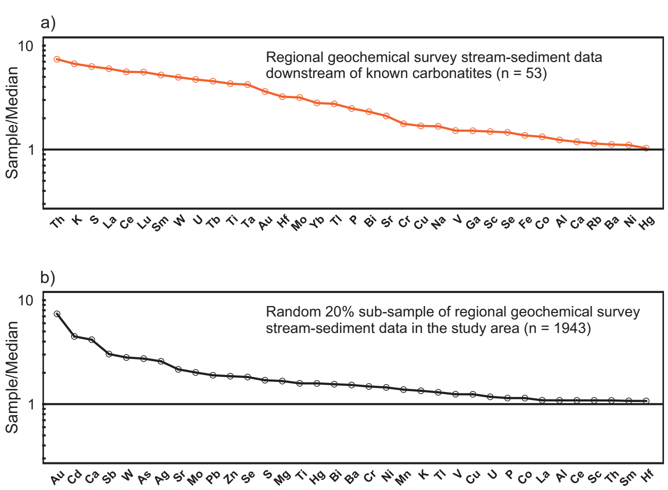

Fig. 14. Ranked element contrast plots relative to the median regional geochemical survey stream-sediment data (Table 4; after Han and Rukhlov, 2017, 2020b). **a)** The average stream-sediment data downstream of known carbonatite or related-rock occurrences. **b)** The average random 20% sub-sample of stream-sediment data.

Table 5. Coefficients for discriminant parameters.

Variable	DP1		DP2	
	Projection[1]	Correlation[2]	Projection[1]	Correlation[2]
log (Ba ppm)	0.5125122	-0.023	1.0080582	0.369
log (Ca wt%)	-0.1132357	0.213	-0.6432403	-0.602
log (K wt%)	0.0190009	-0.458	-0.8340383	0.250
log (Mg wt%)	-0.3508289	0.167	2.0342928	-0.024
log (Mn ppm)	-0.7107679	0.159	-0.1111433	0.119
log (Mo ppm)	-0.7341133	-0.104	-0.2681685	0.191
log (Ni ppm)	-0.8465542	0.004	-0.5128953	0.209
log (P wt%)	-0.8646799	-0.434	-0.2221829	0.034
log (Pb ppm)	0.8482791	0.251	0.3704230	0.073
log (Sc ppm)	1.1082783	-0.233	0.0175719	0.362
log (Sm ppm)	-0.8054578	-0.722	-0.0255307	0.228
log (Sr ppm)	-0.1415442	0.113	-0.7922373	-0.636
log (Th ppm)	-2.7800825	-0.792	-1.4640319	0.140
log (Ti wt%)	-0.1456117	-0.383	1.0353020	0.505
log (U ppm)	0.2233847	-0.648	2.4597713	0.497
log (V ppm)	-0.2578595	-0.102	-0.8935080	0.217
log (Zn ppm)	0.9749035	0.171	0.2481454	0.192
log (La ppm)	-2.1814112	-0.740	0.2285954	0.156
log (Fe wt%)	2.2246271	-0.027	0.5292998	0.188
log (Ce ppm)	1.9567853	-0.718	-0.7624135	0.128
Constant	0.0381130		1.6581413	
Eigenvalue[3]	0.286 (73%)		0.103 (27%)	

[1] Scaled eigenvectors or projection coefficients.
[2] Pearson correlation coefficients between the input data and the projected data indicating contributions of each element in discriminating between groups of samples.
[3] Relative significance of discriminant parameter in terms of eigenvalues of the within-groups sum of squares to between-groups sum of squares ratio matrix and their percentage values (in parentheses).

S_x is the catchment area of stream basin at the sampling site (in m²).
C_x is the concentration of an element in the stream sediment sample (in wt.%).
C_b is the background concentration of an element (in wt.%).

We estimate local background as the geometric mean or median concentration of an element in stream sediment samples (n=20 to 170) that are close to a geochemical anomaly. Downstream of a metal source (secondary dispersion halo), P_x is constant in an ideal dispersion stream, which may not be true for the second- or higher-order drainages (Rukhlov et al., 2020b).

Assuming k=1, the quantity of metal above background or predicted geochemical resources of an element in the stream basin, q (in tonnes per 1 m depth), is calculated as

$$q = H \cdot P_x/40 = P_x/40 \qquad \text{(Eqn. 4)}$$

where

H=1 is the calculation depth (in m).

P_x is the productivity of an element in dispersion stream (in m²%). The denominator '40' converts m²% into tonnes. We set the calculation depth, which refers to a probable depth of a mineralized zone, to a constant value of 1 m to simplify

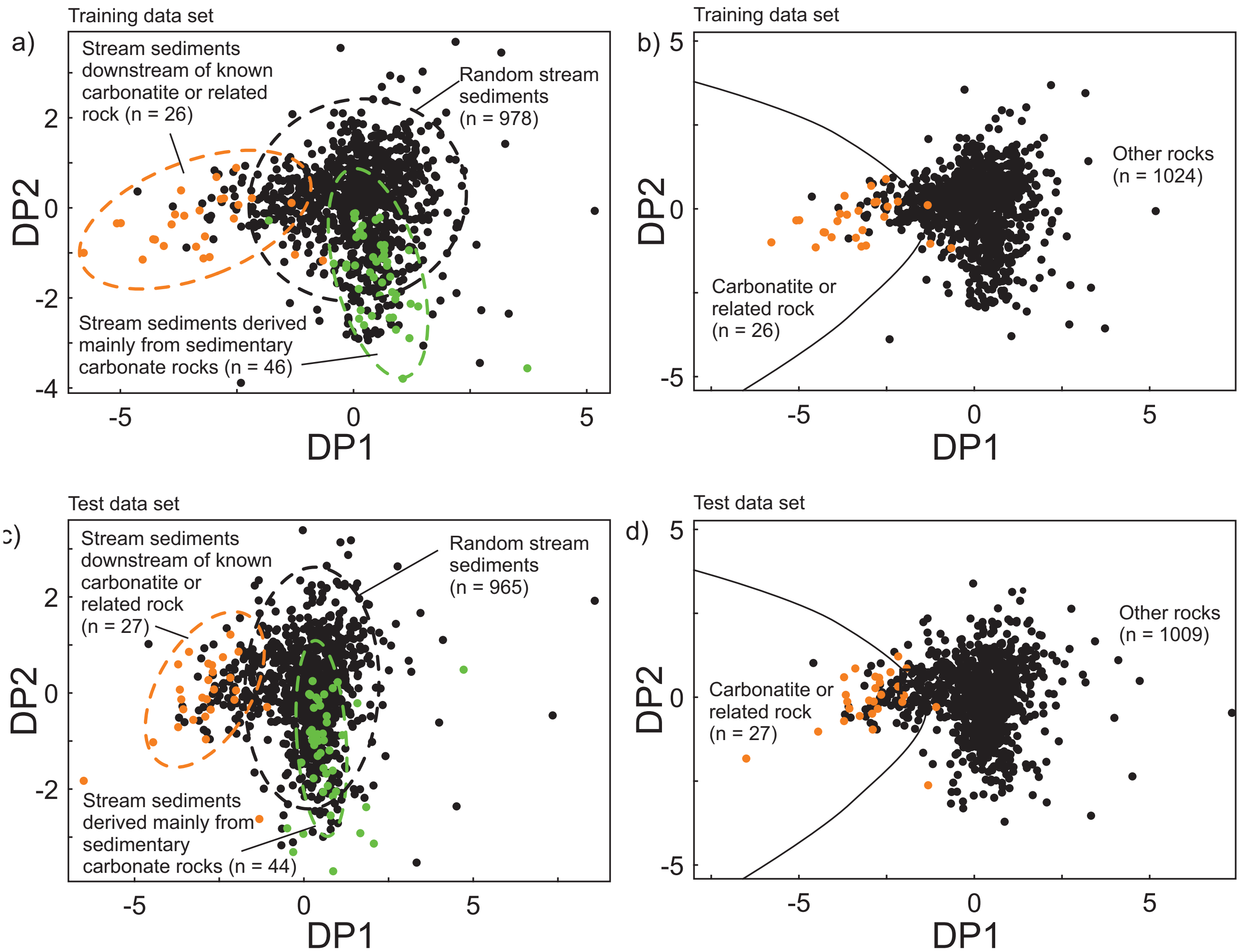

Fig. 15. Discrimination diagram DP1 versus DP2 for regional geochemical survey stream-sediment data. The discriminant-parameter (DP) variables are log10-equivalents of element concentrations in parts per million (ppm) for all elements, except Ca, K, Mg, P, Ti, and Fe which are in weight per cent (wt.%; Table 5). **a)** DP1 versus DP2 for the training data set. **b)** DP1 versus DP2 for the training data set. **c)** DP1 versus DP2 for the test data set (not used in the discriminant analysis). **d)** DP1 versus DP2 for the test data set (not used in the discriminant analysis).

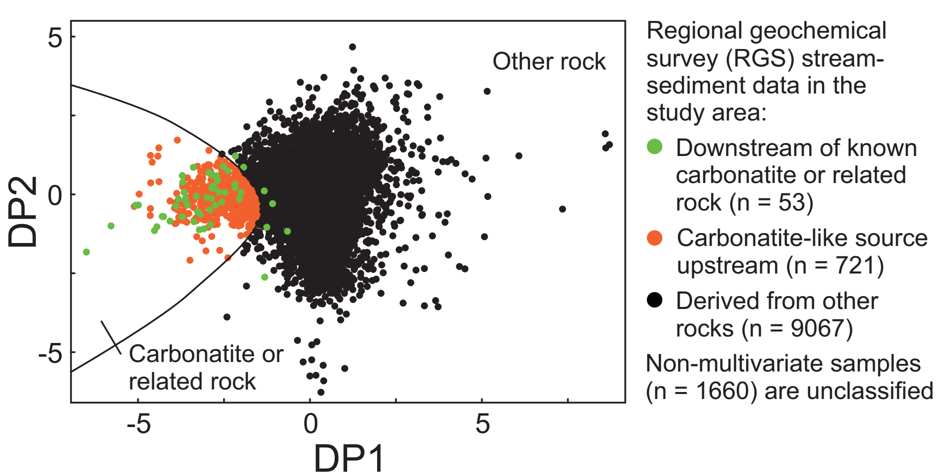

Fig. 16. Discrimination diagram DP1 versus DP2 for all regional geochemical survey stream-sediment data in the study area (after Han and Rukhlov, 2017, 2020b), showing boundary between carbonatite or related-rock sources and other rock sources in the upstream basins. Stream-sediment data downstream of known carbonatite and related-rock occurrences shown separately (green symbols).

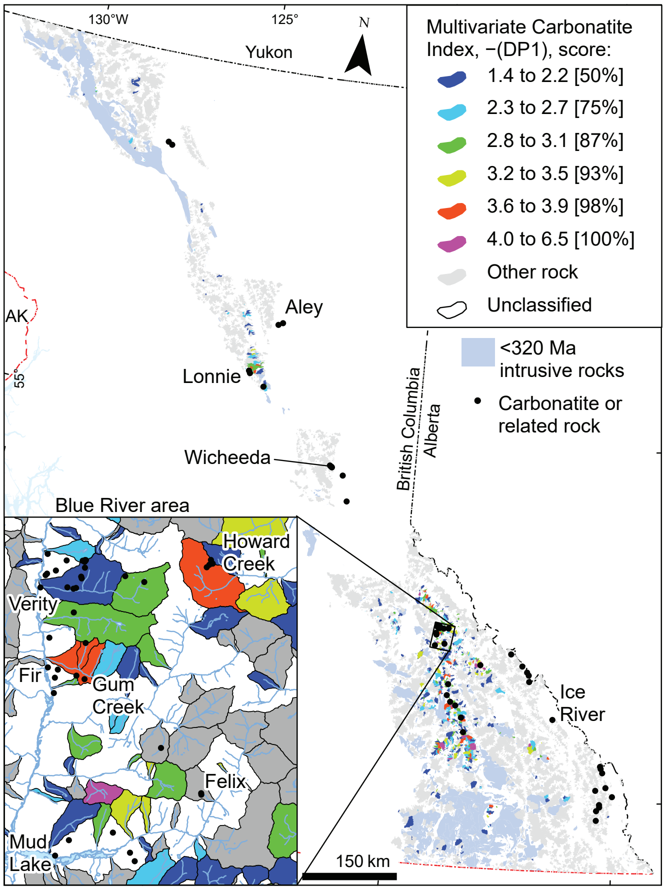

Fig. 17. Carbonatite index-themed, percentile-ranked catchment basins of regional geochemical survey stream-sediment samples (<0.18 mm fraction; after Han and Rukhlov, 2017, 2020b). Carbonatite and related-rock occurrences after Höy (1988), Parrish and Scammell (1988), Pell (1994), Millonig and Groat (2013), and Rukhlov et al. (2018). The post-320 Ma intrusive rocks from BC Digital Geology version 2021-12-19 (Cui et al., 2017).

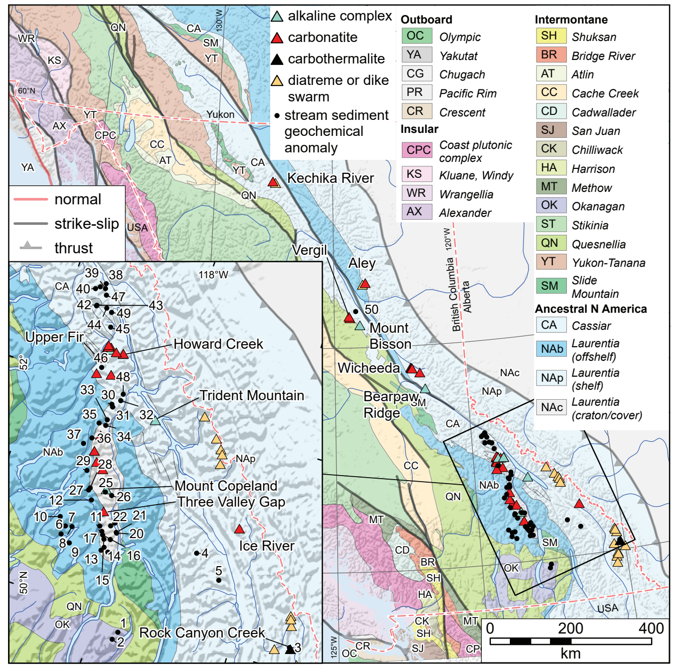

Fig. 18. Stream-sediment geochemical anomalies showing carbonatite index score greater than the 93rd percentile (see Table 6 for locations and other details). Carbonatite and related-rock occurrences after Höy (1988), Parrish and Scammell (1988), Pell (1994), Millonig and Groat (2013), Rukhlov et al. (2018). Terranes after Colpron (2020).

equation 4 for a regional evaluation of geochemical anomalies (see Rukhlov et al., 2020a, b for details about predicted geochemical resources). The estimated predicted geochemical resources (in tonnes of metal per 1 m depth) suggest significant potential for REE and other carbonatite-hosted critical metals in the identified stream basins (Table 6).

7.3. Application to Aley carbonatite complex

Here we use an example of detailed stream-sediment lithogeochemical data downstream of the Aley carbonatite (Mackay and Simandl, 2014) to evaluate the mechanical dispersion of carbonatite indicators and ultimately the utility of the estimated predicted geochemical resources assuming an ideal dispersion (Table 6). Hosted by siliciclastic and carbonate rocks of the Kechika Group (Cambrian to Ordovician), the Aley carbonatite complex (ca. 370 Ma; Fig. 19) contains an NI 43-101-compliant resource of 286 million tonnes (Measured+Indicated) grading 0.37% Nb_2O_5 plus 144 million tonnes (Inferred) grading 0.32% Nb_2O_5 (Jones et al., 2017), making it the largest Nb deposit of the Cordilleran alkaline province (Pride, 1983; Mäder, 1987; McLeish, 2013; Chakhmouradian et al., 2015; McLeish and Johnston, 2019; McLeish et al., 2020). Based on determinations using a portable X-ray fluorescence analyzer (Mackay and Simandl, 2014), concentrations of carbonatite indicator elements such as Nb, La, Y, and Sr in the 0.125 to 0.250 mm fraction of stream sediment decrease exponentially downstream of the carbonatite (Fig. 20). Calculated using equation 3 above, productivities of Nb and Y obey an ideal dispersion law (i.e. P_x≈constant downstream of the anomaly) even in the second- and higher-order drainage system (Fig. 19). In contrast, productivity of La decreases and productivity of Sr increases downstream of the Aley carbonatite (Fig. 20). The main hosts of Nb and Y at Aley are the pyrochlore supergroup, ferrocolumbite, and other Nb-minerals, including euxenite (Chakhmouradian et al., 2015). These minerals are more resistant relative to monazite and REE ±F-carbonate minerals, which are the main hosts of REE at Aley (Mäder, 1987; Mackay and Simandl, 2014; Simandl et al., 2017). The increasing productivity of Sr (Fig. 20d) probably reflects contribution from the carbonate country rocks of the Kechika and Road River groups and the Skoki Formation downstream of the Aley carbonatite complex (Fig. 19). More detailed surveys are needed to evaluate dispersion of critical metals downstream of other known carbonatite and related-rock occurrences, but the data from Aley indicate that resistant critical minerals generally obey an ideal dispersion law even in the high-order streams, thereby validating the estimated predicted geochemical resources (Table 6).

Table 6. Regional geochemical survey stream-sediment data showing carbonatite index scores >93rd percentile and predicted geochemical resources (*q*) of carbonatite-hosted metals (in tonnes per 1 m depth) in stream basins.

N[1]	RGS sample	X[2]	Y[2]	S[3]	CI[4]	Ranked element contrast leaders[5]	Predicted geochemical resources (in tonnes per 1 m depth)[6]															Predominant host rock
							Nb	Ta	La	Ce	Nd	Sm	Eu	Tb	Yb	Lu	Y	Sc	Mo	Th	U	
1	082F775336	-117.623	49.883	25	3.7	W-41, Nb-14, Au-12, U-11, Th-9, Mo-8, La-7, (Ce, Cd)-5, (Sm, Se, Na, Ti, Tl)-3, (K, Te)-2	0	16	13709	19844	na	551	na	16	0	0	0	0	158	4897	983	metamorphic rocks (Harper Ranch assemblage; Carboniferous to Permian)
2	082F775345	-117.670	49.804	3	3.7	Nb-17, Mo-9, K-8, Th-6, (P, La, Ti, Tl)-5, Ce-4, (Y, Hf, Te, W, Sm, U, Cd)-3, (Zr, Ba, V)-2	2.5	0	1019	1528	na	48	na	0.51	0	0	119	0	27	324	na	metamorphic rocks (Harper Ranch assemblage; Carboniferous to Permian)
3	082J901240	-115.162	50.223	2	3.5	Ca-21, Au-14, (Ba, Mo)-13, Sb-11, Mg-10, La-9, (Te, Cd)-8, Tl-7, (Sb, Sr, W)-6, Th-5	2.6	0	936	1749	na	66	na	3.5	0	2.3	86	0	37	185	2.2	limestone, slate, siltstone, argillite (Banff and Exshaw formations; Mississippian)
4	082K775330	-116.879	50.820	19	4.6	Bi-147, Th-82, U-48, Ta-47, Te-29, La-23, Nb-22, W-19, (Hf, V, Zr, Tb)-6, Ce-5, (Fe, Na, Y)-3	280	3257	24198	16529	na	712	na	219	0	0	682	0	17	22111	10485	coarse siliciclastic rocks (Horsethief Creek Group; Neoproterozoic)
5	082K777088	-116.445	50.639	13	3.6	W-158, Nb-22, U-17, Ta-11, Th-9, La-7, U*-6, Mo-5, F*-4, (Ce, P, Y, Na)-3, (Bi, Rb, Cs)-2	192	502	3531	4663	na	55	na	3.3	0	0	447	0	67	1785	1916	quartzite, quartz arenite (Purcell Supergroup, Mount Nelson and Dutch Creek formations; Mesoproterozoic)
6	082L763159	-118.876	50.589	15	3.7	Th-13, Ce-8, (Sm, Hf, Zr, Lu, La, Tb)-6, U-5, (W, Na)-4, (Cr, Ti)-3, (Ta, K, Sc, P, S, Yb)-2	na	54	7931	19105	na	1261	na	144	37	59	na	218	0	4979	553	limestone, marble, calcareous sedimentary rocks (Shuswap assemblage; Proterozoic to Paleozoic)
7	082L763165	-118.855	50.674	23	3.6	(Au, Th)-11, Lu-8, Sm-7, (Ce, La, W)-6, (Tb, Hf, U, Na)-5, (Zr, Ti)-4, (Cr, K, Yb, Sc, Ta)-3	na	125	14252	23051	na	2071	na	205	289	139	na	771	0	6184	757	limestone, marble, calcareous sedimentary rocks (Shuswap assemblage; Proterozoic to Paleozoic)
8	082L763168	-118.759	50.688	69	5.0	Au-56, W-54, Th-23, Lu-19, Sm-13, La-12, (U, Tb)-11, (Ce, Hf)-9, Zr-8, (Na, Yb)-4, (Ta, Cr)-3	na	562	96127	106998	na	14985	na	1690	1202	1185	na	1743	0	47411	7265	limestone, marble, calcareous sedimentary rocks (Shuswap assemblage; Proterozoic to Paleozoic)
9	082L763198	-118.717	50.535	20	5.1	Au-50, Th-25, Lu-22, La-17, (Sm, Ce)-15, U-14, Tb-12, (Hf, Zr)-11, W-7, Na-6, Cr-5, Yb-4	na	135	38930	58564	na	4990	na	529	439	381	na	583	0	15229	2753	quartzite, quartz arenite (Shuswap assemblage; Proterozoic to Paleozoic)
10	082L765210	-118.973	50.742	14	3.8	Th-9, Zr-8, (Hf, Ce, La, Sm)-6, Lu-5, (U, Tb, Na)-4, (K, Ti, Cr)-3, (Na, P, Ba, Yb, Sc, Tl)-2	na	0	6794	11991	na	941	na	86	34	34	na	52	0	2663	384	metamorphic rocks (Shuswap assemblage; Proterozoic to Paleozoic)
11	082L765223	-118.372	50.778	46	3.6	W-34, Th-10, (Zr, Ce, La)-8, Sm-7, (Hf, Lu, Na)-6, (U, Tb, Ti, K)-5, (Cr, Yb)-3, (Sc, P, Tl)-2	na	129	30216	49718	na	3647	na	229	228	114	na	1197	25	9061	976	limestone, marble, calcareous sedimentary rocks (Shuswap assemblage; Proterozoic to Paleozoic)

[1] Anomaly number as shown in Fig. 18.
[2] Longitude (X) and latitude (Y) coordinates (in decimal degrees) of regional geochemical survey (RGS) stream sediment sample.
[3] Area of catchment basin (in km^2).
[4] Carbonatite index (CI) score values; CI = −DP1 (Table 5).
[5] Ranked element contrast (REC) leaders are sorted (maximum to minimum) element concentrations normalized to the median values of regional geochemical survey stream-sediment data (Table 4). REC leaders reveal associations of elements showing the maximum contrast to background and the magnitude of the contrast (geochemical anomaly), which identify mineralization in the stream basin. Anomalies 1 to 37 and 50 lack Nd and Eu determinations; anomalies 6 to 50 lack Nb and Y determinations. F* and U* are fluorine and uranium determinations in stream water. **na** = not analyzed.
[6] Predicted geochemical resources in the stream basin (in tonnes of metal per 1 m depth); see text for details.

Table 6. Continued.

N[1]	RGS sample	X[2]	Y[2]	S[3]	CI[4]	Ranked element contrast leaders[5]	Predicted geochemical resources (in tonnes per 1 m depth)[6]															Predominant host rock
							Nb	Ta	La	Ce	Nd	Sm	Eu	Tb	Yb	Lu	Y	Sc	Mo	Th	U	
12	082L765268	-118.616	50.985	3	3.9	(Th, W) -12, Lu-10, (U*, La, Ce)-8, Sm-7, (U, Tb)-6, Yb-5, (Hf, F*, Zr)-4, (Ta, W, Na, Ti)-3	na	20	2006	3606	na	236	na	26	68	24	na	57	0	841	115	coarse siliciclastic rocks (Horsethief Creek Group; Neoproterozoic)
13	082L769008	-118.239	50.566	9	3.6	(K, Th)-10, (W, Lu)-9, (Na, Ce)-7, (Ti, La, Tb, Zr, Sm, U, Tl)-6, Hf-5, Cr-4, (Yb, Sc, P)-3, Ga-2	na	27	4072	6882	na	538	na	76	87	50	na	155	8.0	1600	282	quartzite, quartz arenite (Monashee complex; Proterozoic to Early Paleozoic)
14	082L769010	-118.210	50.602	16	3.5	W-18, Th-8, Lu-7, (Ce, U, Tb, Sm, La)-5, (Yb, Au, K, Zr)-4, (Na, Ti, Hf)-3, (Tl, P, Cr, Na)-2	na	21	4561	8113	na	649	na	101	282	52	na	121	0	2198	394	quartzite, quartz arenite (Monashee complex; Proterozoic to early Paleozoic)
15	082L769070	-118.252	50.674	7	4.4	(Lu, Th)-16, W-14, U-12, Tb-11, Sm-10, (Ce, La)-9, Yb-7, Au-6, (K, Zr)-5, (Hf, Na)-4, Ti-3	na	9.3	6323	10626	na	934	na	153	263	91	na	35	0	2871	726	quartzite, quartz arenite (Monashee complex; Proterozoic to early Paleozoic)
16	082L769071	-118.290	50.707	3	4.4	Lu-24, Th-22, U-16, Tb-15, (La, Sm, Ce)-13, Yb-10, Zr-7, (W, Hf)-6, K-5, (Cr, Ti)-4, Na-3	na	12	4920	7943	na	690	na	111	209	71	na	64	0	2103	540	quartzite, quartz arenite (Monashee complex; Proterozoic to early Paleozoic)
17	082L769075	-118.319	50.738	4	3.9	W-23, Th-17, Tb-12, (Lu, U)-11, Sm-10, (La, Ce)-9, Ti-7, (Zr, Yb)-6, Hf-5, (Au, Rb, Ba)-4	na	30	3495	5656	na	581	na	99	122	33	na	82	7.3	1788	379	quartzite, quartz arenite (Monashee complex; Proterozoic to early Paleozoic)
18	082L769153	-118.135	50.570	7	3.9	W-30, Lu-17, Yb-12, (Th, U)-11, Tb-9, (U, Ce)-8, (Sm, Na, La)-7, (Zr, Hf)-5, (Ti, K, P)-3	na	5.5	3583	7419	na	530	na	113	488	89	na	153	0	1539	376	orthogneiss (Paleoproterozoic)
19	082L769158	-118.160	50.690	5	3.7	(Th, Lu)-13, W-12, (Tb, Ce)-9, (Sm, La)-8, U-7, (Yb, Au)-6, Hf-5, (Zr, K, Na)-4, (Cr, Ti, Tl)-2	na	2.7	3294	6338	na	524	na	80	155	47	na	36	0	1497	198	paragneiss (Paleoproterozoic)
20	082L769159	-118.102	50.766	57	4.6	W-19, Th-15, Lu-13, Sm-9, (Tb, Ce, La)-8, U-7, Yb-6, Hf-5, Zr-4, (Na, Ba, Rb, Au)-2	na	61	37810	66635	na	7103	na	857	1569	542	na	0	0	21751	2447	quartzite, quartz arenite (Monashee complex; Proterozoic to early Paleozoic)
21	082L769160	-118.110	50.771	37	4.6	Th-20, Lu-16, (Tb, W)-14, Sm-12, U-10, (La, Ce)-9, Yb-7, (Zr, S)-5, Hf-4, (Na, K, As)-3	na	143	34167	52331	na	6785	na	1096	1404	477	na	0	0	20635	2963	Paragneiss (Paleoproterozoic)
22	082L769169	-118.220	50.813	10	4.6	Lu-21, Th-20, (La, Sm)-13, (Ce, Hf, Tb)-12, (U, K)-11, Zr-10, Yb-7, Ti-6, Tl-5, Cr-4, (Na, Sc)-3	na	0	13707	22151	na	1944	na	241	372	174	na	171	8.7	5251	933	quartzite, quartz arenite (Monashee complex; Proterozoic to early Paleozoic)
23	082L769171	-118.174	50.851	34	3.5	Th-6, (Zr, Hf)-5, (Lu, Sm, Tb, Ce)-4, (U, La, K, Na)-3, (W, Ti, P, Yb, Ta)-2	na	46	1126	1048	na	653	na	70	0	26	na	0	0	2303	83	calc-silicate metamorphic rocks (Monashee complex; Proterozoic to early Paleozoic)
24	082L769172	-118.174	50.851	34	3.6	W-27, Th-6, (Zr, Hf)-5, (Ce, Lu, Sm)-4, (La, Tb, U, Na)-3, (K, Yb, P, Ti)-2	na	28	1985	7064	na	464	na	27	0	17	na	0	0	2157	0	calc-silicate metamorphic rocks (Monashee complex; Proterozoic to early Paleozoic)
25	082M763128	-118.457	51.098	4	3.6	Mo-159, Na-11, W-8, (K, Ti)-7, (La, F*, Au, U, Zr)-6, (Hf, Ta, Ce, Sr, Th)-4, (P, Ga, Tl)-3	na	44	1083	1748	na	38	na	6.5	20	4.0	na	0	837	48	65	calc-silicate metamorphic rocks (Monashee complex; Proterozoic to early Paleozoic)

Table 6. Continued.

N[1]	RGS sample	X[2]	Y[2]	S[3]	CI[4]	Ranked element contrast leaders[5]	Predicted geochemical resources (in tonnes per 1 m depth)[6]															Predominant host rock
							Nb	Ta	La	Ce	Nd	Sm	Eu	Tb	Yb	Lu	Y	Sc	Mo	Th	U	
26	082M763135	-118.351	51.086	41	3.9	W-45, Mo-18, Zr-11, Hf-8, (Na, Th, La, Ce)-6, (Ta, U)-5, (Lu, F*, Sm, K, Ti, Tb)-4, Sr-3	na	531	19006	32392	na	1504	na	147	405	111	na	0	861	4263	983	calc-silicate metamorphic rocks (Monashee complex; Proterozoic to early Paleozoic)
27	082M767025	-118.703	51.065	4	4.6	Th-15, La-12, Ce-9, Sm-7, (Hf, P)-6, (Tb, Zr)-5, (U, Ti)-4, (Na, K)-3, (Cr, W, Ca, Ga, Ba, Ta)-2	na	1.3	4724	5753	na	351	na	31	0	0	na	0	0	1616	80	coarse siliciclastic rocks (Horsethief Creek Group; Neoproterozoic)
28	082M767028	-118.692	51.089	14	3.9	Th-9, W-8, (La, Na)-7, Ce-6, Sm-5, (Au, Ti, Zr)-4, (Tb, Hf, K, S, U)-3, (P, Sc, Sr, Mo)-2	na	0	9233	12010	na	671	na	49	0	0	na	120	0	3079	54	calc-silicate metamorphic rocks (Monashee complex; Proterozoic to early Paleozoic)
29	082M769045	-118.823	51.234	59	3.5	W-24, Na-9, (Th, Sm, Tb)-5, (K, Zr, Ti, La, Ce)-4, (Hf, Ta, U, Lu)-3, (Cr, P, Tl, Yb, Mo, Au)-2	na	150	12964	20801	na	3031	na	339	0	67	na	201	0	5753	223	calc-silicate metamorphic rocks (Monashee complex; Proterozoic to early Paleozoic)
30	082M775247	-118.797	51.898	22	3.6	W-198, Na-12, (Lu, Th)-10, (Tb, Ce)-9, Sm-8, (La, U)-7, (Ta, Yb)-5, (Bi, Au, Cr, Ti, Zr)-4	na	282	13883	32403	na	2392	na	376	485	172	na	386	0	5005	1093	limestone, marble, calcareous sedimentary rocks (Horsethief Creek Group; Neoproterozoic)
31	082M775249	-118.772	51.876	30	3.7	Lu-13, Th-12, Tb-10, (Sm, Ce)-9, (W, La)-8, (Na, U)-7, (Zr, Yb)-5, Hf-4, (Ti, Ta, K)-3, Cr-2	na	146	21534	49050	na	4092	na	603	832	318	na	414	0	9598	1542	limestone, marble, calcareous sedimentary rocks (Horsethief Creek Group; Neoproterozoic)
32	082M775264	-118.687	51.958	8	3.7	Th-9, (Tb, Sm, W)-8, (Zr, Lu)-7, (Na, U, La)-6, (Ce, Hf)-5, (Ta, Yb, K, Ti)-4, (Cr, Au, Sc, P)-2	na	78	3439	4349	na	845	na	125	162	34	na	161	0	1619	304	limestone, marble, calcareous sedimentary rocks (Horsethief Creek Group; Neoproterozoic)
33	082M775405	-118.786	51.746	4	3.7	W-12, (Th, Na)-8, Au-6, (Sm, Tb)-5, (La, Ti, Ce)-4, (K, Ta, U, Mo)-3, (Cr, Hf, Zr, Sc, P)-2	na	15	917	1358	na	167	na	20	0	0	na	28	6.4	590	19	limestone, marble, calcareous sedimentary rocks (Horsethief Creek Group; Neoproterozoic)
34	082M775408	-118.779	51.692	15	3.8	Th-8, (Na, La, Zr, Sm)-6, (Hf, Ce, Tb, K)-5, (Ti, U, Cr, Lu)-4, Ta-3, (Yb, P, W, Tl, Sc)-2	na	85	7017	9210	na	915	na	87	73	22	na	109	0	2632	293	limestone, marble, calcareous sedimentary rocks (Horsethief Creek Group; Neoproterozoic)
35	082M775413	-118.887	51.692	20	3.8	Au-14, Th-10, Zr-8, (Sm, Hf, Tb, Lu)-7, (La, Na, Ce)-6, (W, U)-5, (K, Yb)-4, Ti-3, (Cr, Ta)-2	na	26	10734	14754	na	1855	na	210	294	83	na	308	0	4952	540	limestone, marble, calcareous sedimentary rocks (Horsethief Creek Group; Neoproterozoic)
36	082M775470	-118.916	51.538	5	4.1	W-15, Th-12, (La, Ce, Sm)-8, Tb-7, Lu-6, (Ti, U)-5, (Na, K, Ta)-4, (Cr, Hf, Zr, Yb, Au)-3	na	31	3671	6367	na	501	na	57	35	19	na	35	0	1406	129	coarse siliciclastic rocks (Horsethief Creek Group; Neoproterozoic)
37	082M775479	-119.007	51.463	18	3.8	(Th, Lu)-8, W-7, (Sm, Tb)-6, (La, Ce, Zr, Hf)-5, (U, Na)-4, (Yb, S, Cr)-3, (Ti, K, Ta)-2	na	0	7286	11239	na	1152	na	149	220	92	na	43	0	3205	352	coarse siliciclastic rocks (Horsethief Creek Group; Neoproterozoic)
38	083D051004	-119.499	52.949	0.3	3.5	S-17, Th-6, (La, K)-5, (Ta, Hf, Sm, Ce, Eu)-4, (Cu, U, Lu, Tl)-3, (Yb, Na, Ti, P, Bi, Tb, Te)-2	na	1.2	61	68	0	6.4	1.9	0	0.21	0.07	na	na	0.08	21	2.7	dolomitic carbonate rocks (Rocky Mountain assemblage; middle Cambrian)
39	083D051005	-119.484	52.904	7	3.6	Th-8, Ta-7, (La, Ce, K, Sm)-6, (Lu, Yb, U)-5, (Hf, Nd, Tb)-4, (Tl, P, Eu, Ti, W, F*, Na, Sc)-3	na	89	2892	5332	2006	352	32	26	135	17	na	195	4.2	973	184	mudstone, siltstone, shale (Kaza Group, lower division; Neoproterozoic)

Table 6. Continued.

N[1]	RGS sample	X[2]	Y[2]	S[3]	CI[4]	Ranked element contrast leaders[5]	Predicted geochemical resources (in tonnes per 1 m depth)[6]															Predominant host rock
							Nb	Ta	La	Ce	Nd	Sm	Eu	Tb	Yb	Lu	Y	Sc	Mo	Th	U	
40	083D051070	-119.630	52.872	16	4.4	Ti-34, (Hf, Th)-13, (Ce, La, K, Sm)-10, (Au, U)-9, S-8, Tb-7, (Nd, Eu)-6, (Ta, Cu, Lu, Yb)-5	na	136	14860	27435	10643	2083	276	211	280	35	na	59	26	5211	1261	mudstone, siltstone, shale (Kaza Group, lower division; Neoproterozoic)
41	083D051077	-119.569	52.903	3	3.5	Th-10, (La, Ce)-8, (Lu, Yb, Sm, K)-7, (Tb, Ta)-6, (U, Nd)-5, (Eu, Te, Tl, Hf, Ti)-4, (Sc, Fe)-3	na	24	1631	2936	1132	215	23	25	97	13	na	130	0	561	80	coarse siliciclastic rocks (Kaza Group; Neoproterozoic)
42	083D051144	-119.525	52.723	2	3.8	K-10, (La, Ti, Ta, Th)-5, (Sm, Ce, Eu, P, Tl)-4, (Tb, Na, U, Cu, Yb, Mo)-3, (Hf, Ba, Cr, Nd)-2	na	13	510	399	43	40	14	4.9	5.1	0.43	na	8.5	3.4	74	13	mudstone, siltstone, shale (Horsethief Creek Group, lower pelite unit; Neoproterozoic)
43	083D051145	-119.522	52.729	4	3.7	Au-35, Th-6, La-5, (Ce, Sm, K, Ta)-4, (Tb, Eu, U, Ti, Hf, Tl, W)-3, (Lu, Yb, Se, Nd, Te, Na)-2	na	17	1163	1183	196	99	21	11	1.0	na	na	0	2.9	267	39	mudstone, siltstone, shale (Kaza Group, lower division; Neoproterozoic)
44	083D051157	-119.363	52.735	6	3.7	Th-8, (K, La)-7, (Sm, Ce, Ta)-6, U-5, (Tb, Ti, Lu, Yb, Hf, Eu)-4, (Tl, Te, Sc, Na, Co, Nd)-3	na	54	2928	3646	563	364	36	32	72	9.9	na	183	0	960	155	mudstone, siltstone, shale (Kaza Group, lower division; Neoproterozoic)
45	083D051371	-119.206	52.579	2	3.7	Th-7, (La, Ce)-6, (Sm, U)-5, (K, Tb, Hf)-4, (Nd, Tl, Eu, Ta, Ti, Lu)-3, (Bi, F*, Yb, Te, Na, Fe)-2	na	0	790	1392	455	108	6.2	11	0	0	na	0	0	266	63	mudstone, siltstone, shale (Kaza Group, lower division; Neoproterozoic)
46	083D051424	-119.131	52.193	8	3.9	K-12, (La, Th)-8, (Ti, Ce)-7, Sm-6, (Tb, U)-5, (Yb, Lu, Tl, Hf, Na, Te, Mo, Eu)-4, (S, Cr)-3	na	6.0	5528	6940	1248	476	58	33	85	9.2	na	15	12	1180	187	metamorphic rocks (Mica Creek succession; Neoproterozoic)
47	083D052034	-119.436	52.848	22	3.5	Th-10, (Ce, La, Bi)-8, Sm-7, (U, K, Nd, Tb)-6, (Ta, Lu)-5, (Hf, S, Yb, Eu)-4, (W, Tl, Ti, Sc)-3	na	181	13570	28871	12285	1996	161	193	285	50	na	580	0	4870	949	quartzite, quartz arenite (Neoproterozoic)
48	083D052128	-118.683	52.022	2	3.9	Th-12, Ce-10, (La, Sm)-9, (Na, Tb, Nd, Hf)-7, (U, Lu)-6, (K, Eu, Yb)-5, Ti-4, W-3, (P, Sc)-2	na	0	2225	4410	1718	307	29	29	53	7.7	na	45	0	692	101	metamorphic rocks (Mica Creek succession; Neoproterozoic)
49	083D053028	-119.270	52.712	15	3.5	Th-11, Ce-10, (La, Sm)-9, U-7, (Ta, Nd, Tb, K, W)-6, (Hf, Lu, Yb)-5, (Eu, Ti)-4, (Tl, Sc, Fe)-3	na	185	12849	25279	9914	1718	145	139	271	38	na	572	0	4202	763	mudstone, siltstone, shale (Kaza Group, lower division; Neoproterozoic)
50	093N831597	-124.151	55.812	13	3.8	P-13, Th-9, (Lu, Ce)-6, (Sm, Au, La, U, Na)-5, (Zr, Tb)-4, (Hf, K)-3, (Ti, Te, Tl, Ta, Yb, Cr)-2	na	20	3805	6842	na	624	na	52	33	50	na	0	0	1911	118	argillite, greywacke, wacke, conglomerate (Ingenika Group, Swannell Formation; Neoproterozoic)

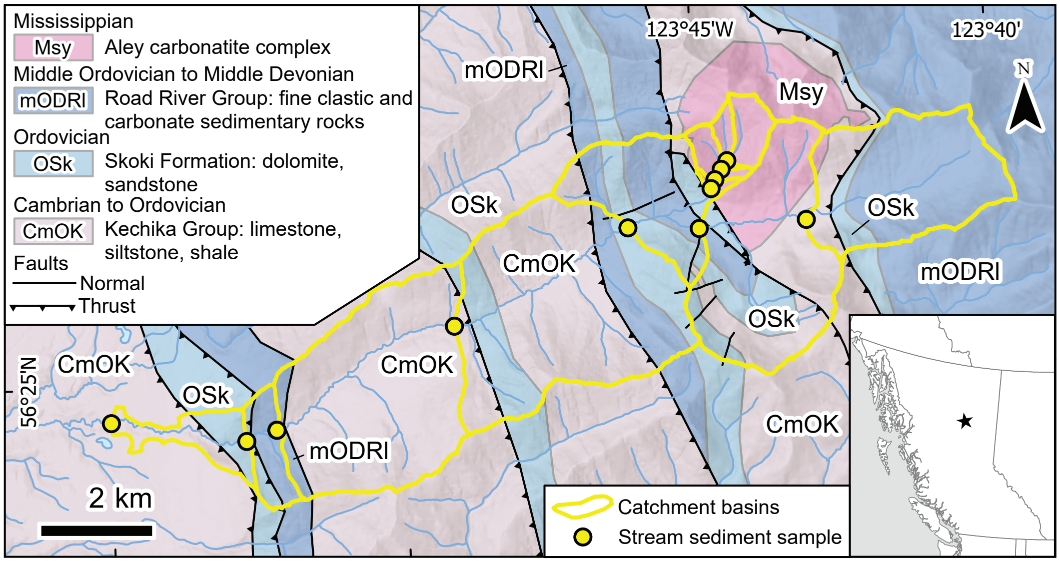

Fig. 19. Sampling sites and catchment basins at Aley carbonatite complex. Sampling sites after Mackay and Simandl (2014). Geology after Pride (1983), Mäder (1987), McLeish (2013), and BC Digital Geology version 2021-12-19 (Cui et al., 2017).

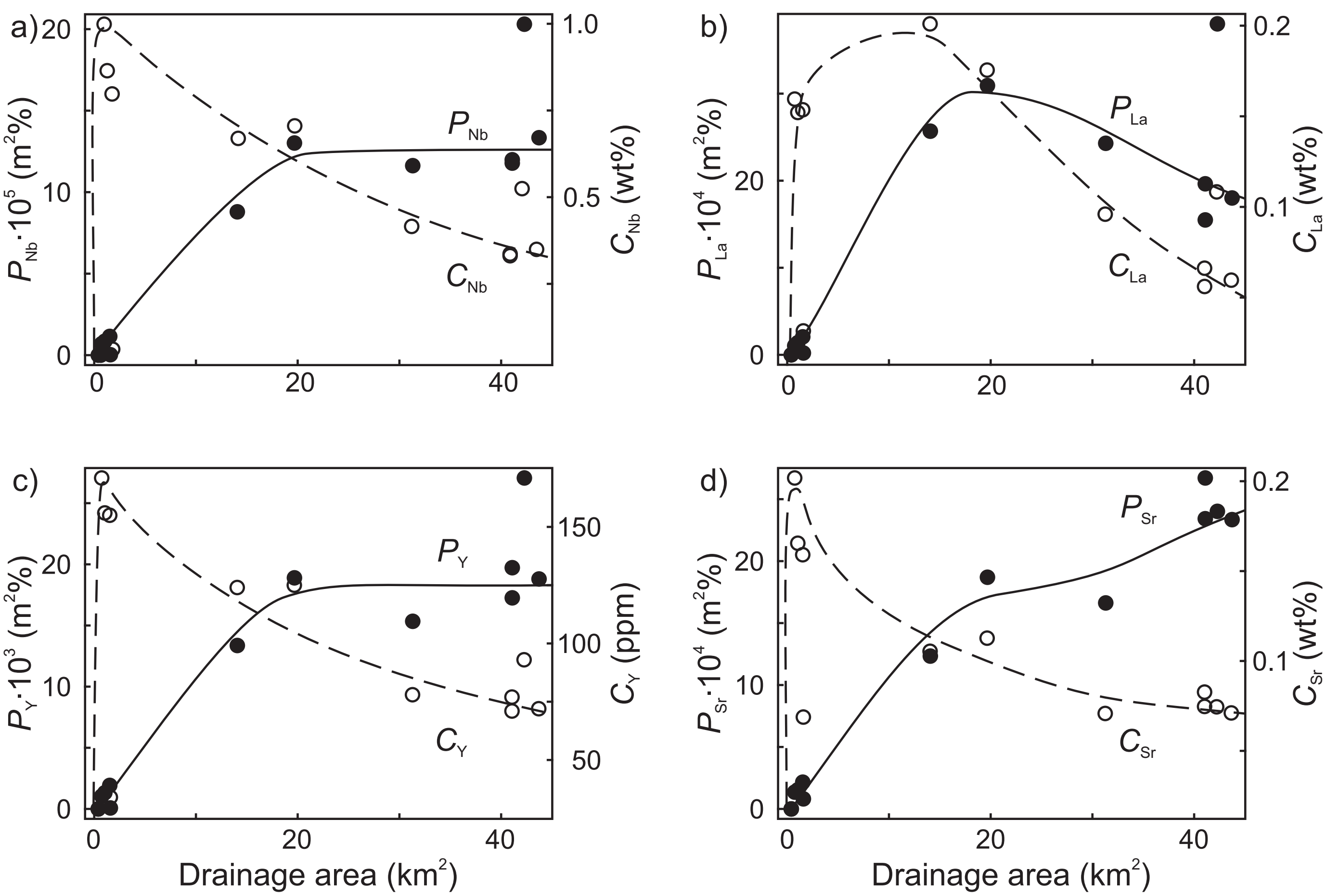

Fig. 20. Aley carbonatite complex, drainage area (km^2) versus concentration, C_x (wt.% or ppm; open symbols; model dashed line), and productivity, P_x (m^2%; solid symbols, model solid line), of selected elements for the 0.125 to 0.250 mm fraction of stream-sediment samples. Original concentrations from Mackay and Simandl (2014). **a)** Drainage area (km^2) versus C_{Nb} (wt.%) and $P_{Nb}\cdot 10^5$ (m^2%). **b)** Drainage area (km^2) versus C_{La} (wt.%) and $P_{La}\cdot 10^4$ (m^2%). **c)** Drainage area (km^2) versus C_Y (ppm) and $P_Y\cdot 10^3$ (m^2%). **d)** Drainage area (km^2) versus C_{Sr} (wt.%) and $P_{Sr}\cdot 10^4$ (m^2%).

8. Discussion

Based on data from known carbonatites, an integrated approach to assess the critical metals potential of underexplored regions might combine detailed stream-sediment sampling and application of the critical mineral index as defined herein, high-resolution airborne radiometric and magnetic data, and panned heavy mineral concentrate and soil lithochemical surveys.

8.1. Geophysical response from carbonatites of the Blue River area

Both airborne radiometric and magnetic surveys are effective prospecting tools for carbonatite-hosted critical minerals (e.g., Simandl and Paradis, 2018), many of which contain U and Th and are associated with abundant magnetic minerals such as magnetite or pyrrhotite and K-rich metasomatic rocks such as glimmerites (carbonate-amphibole-phlogopite rocks). High-resolution, airborne gamma-ray uranium (Fig. 21) and total magnetic intensity (Fig. 22) highs highlight numerous known carbonatite occurrences in the Blue River area, which illustrate the effectiveness of geophysics for critical minerals prospecting, especially in vegetated, low-elevation areas (Gorham, 2008; Shives, 2009). However, difficulty in maintaining constant ground clearance in rugged terrain results in gamma counts and total magnetic intensities that reflect topography, with generally stronger responses from ridges and peaks relative to low-elevation areas (Gorham, 2008).

8.2. Stream-sediment, panned heavy mineral concentrate and soil lithochemical surveys

Concentrations of carbonatite indicator elements such as Ba, Mo, Nb, Ta, REE, Th, and U in stream-sediment heavy mineral concentrate (HMC) samples are up to two orders of magnitude higher relative to those in carbonatites and soil samples, and up to 192 times higher relative to the bulk stream-sediment <0.18 mm fraction (Table 3). Recovered by panning in the field or by laboratory techniques (Lett and Rukhlov, 2017), HMC lithogeochemistry enhances the contrast of stream-sediment anomalies compared to the conventional, bulk <0.18 mm fraction used in the RGS drainage programs (Rukhlov et al., 2020a, b). Panned, stream-sediment HMC samples in the Blue River area (n=626), containing 1.2 to 2475 ppm Ta determined by lithium-fusion ICP-MS (Fig. 6), highlight the known carbonatites in the area, including at the Upper Fir and Verity Ta-Nb deposits (Dahrouge and Reeder, 2001; Reeder and Dahrouge, 2002; Smith and Dahrouge, 2003; Dahrouge and Wolbaum, 2004; Rukhlov and Gorham, 2007; Gorham, 2008; Gorham et al., 2009, 2011a, 2011b). In contrast, the RGS stream-sediment data in the area (n=208) show only <1 to 13 ppm Ta by INAA (Fig. 5). In addition, HMC are routinely evaluated for indicator minerals (e.g., Tyson, 2009; Mackay and Simandl, 2014; Mao et al., 2016; Simandl et al., 2017).

As follow-ups to regional stream-sediment and airborne geophysical surveys, grid soil lithogeochemical surveys (Fig. 7), coupled with ground (in situ) gamma-ray and magnetic surveys, effectively delineate secondary (residual) dispersion haloes of carbonatite-related critical metals (Reeder and Dahrouge, 2002; Smith and Dahrouge, 2003; Dahrouge and Wolbaum, 2004; Rukhlov and Gorham, 2007; Gorham, 2008; Gorham et al., 2009, 2011a, 2011b).

9. Conclusion

Carbonatites and related rocks have a very distinct geochemical signature, characterized by extreme concentrations of critical metals such as REE, Nb, Ta and other elements. Because most carbonatites in British Columbia form small sills and dikes, the task of detecting their signal using the

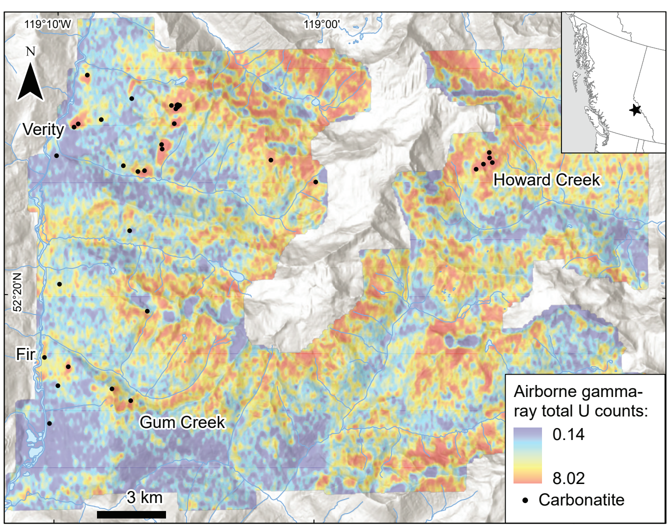

Fig. 21. Blue River area gridded airborne gamma-ray uranium response (total counts). After Gorham (2008) and Shives (2009). Grid cell size is 40 m. Carbonatite occurrences after Rukhlov and Gorham (2007), Gorham (2008), Gorham et al., 2009, 2011a, 2011b, 2013), Millonig and Groat (2013), and Rukhlov et al. (2018).

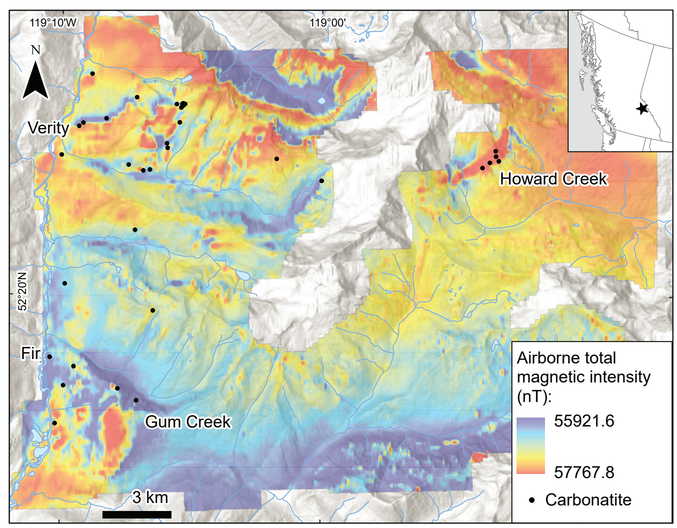

Fig. 22. Blue River area gridded airborne total magnetic intensity response (nT). After Gorham (2008) and Shives (2009). Grid cell size is 40 m. Carbonatite occurrences after Rukhlov and Gorham (2007), Gorham (2008), Gorham et al., 2009, 2011a, 2011b, 2013), Millonig and Groat (2013), and Rukhlov et al. (2018).

multi-element regional geochemical survey stream data with sample catchment areas of up to 193 km^2 (average 10 km^2) is akin to looking for a needle in a haystack. Univariate data reflect background variations, including at known carbonatite and related-rock occurrences. In contrast, our multivariate carbonatite index identifies numerous stream basins that are prospective for carbonatite-related critical minerals. The top 50 anomalies (>93rd percentile) show maximum contrast of carbonatite indicator elements relative to the background in the study area. Estimated predicted geochemical resources suggest significant potential for REE and other carbonatite-related critical metals. We propose a refined prospectivity approach to assess the critical metals potential of underexplored regions that includes stream-sediment, panned heavy mineral concentrate lithochemical and indicator mineral surveys, coupled with high-resolution airborne radiometrics and magnetics, followed up by soil lithochemical and in situ (ground) radiometric and magnetic surveys.

Acknowledgments

We thank Purple Rock Inc. for capturing digital data from the provincial ARIS and Kaitlyn McLaren (British Columbia Geological Survey) for GIS support and data management. We also thank Christopher H. Gammons (Montana Tech of The University of Montana), Kathryn E. Watts (United States Geological Survey), and Lawrence B. Aspler (British Columbia Geological Survey) for thorough reviews and comments.

References cited

Bond, G.C., and Kominz, M.A., 1984. Construction of tectonic subsidence curves for the early Paleozoic miogeocline, Southern Canadian Rocky Mountains: Implications for subsidence mechanisms, age of breakup and crustal thinning: Geological Society of America Bulletin, 95, 155-173.

Burgess, S.D., Heaman, L.M., and Bowring, S.A., 2023. High-precision ID-TIMS U-Pb geochronology of perovskite ($CaTiO_3$) from the Ice River Complex, Southeastern British Columbia. Chemical Geology, 616, article 121187. <https://doi.org/10.1016/j.chemgeo.2022.121187>

Brown, J.A., 2013. Waterloo Resources Ltd. 2012 field activities at the Ice River property, Waterloo Prospect area. British Columbia Ministry of Energy, Mines and Natural Gas, British Columbia Geological Survey, Assessment Report 33565, 39 p.

Brummer, J.J., Gleeson, C.F., and Hansuld, J.A., 1987. A historical prospective of exploration geochemistry in Canada. Journal of Geochemical Exploration, 28, 1-39.

Campbell, N.A., 1980. Robust procedures in multivariate analysis. I: Robust covariance estimation. Journal of the Royal Statistical Society, Series C: Applied Statistics, 29, 231-237.

Campbell, R.B., 1968. Geology, Canoe River, British Columbia. Geological Survey of Canada, Preliminary Map 15-1967, 1:253,400 scale.

Chakhmouradian, A.R., Reguir, E.P., Kressall, R.D., Crozier, J., Pisiak, L.K., Sidhu, R., and Yang, P., 2015. Carbonatite-hosted niobium deposit at Aley, northern British Columbia (Canada): Mineralogy, geochemistry and petrogenesis. Ore Geology Reviews, 64, 642-666.

Chudy, T.C., 2013. The petrogenesis of the Ta-bearing Fir carbonatite system, east-central British Columbia, Canada. Unpublished Ph.D. thesis, University of British Columbia, Canada, 316 p.

Çimen, O., Kuebler, C., Simonetti, S.S., Corcoran, L., Mitchell, R.H., and Simonetti, A., 2019. Combined boron, radiogenic (Nd, Pb, Sr), stable (C, O) isotopic and geochemical investigations of carbonatites from the Blue River Region, British Columbia (Canada): Implications for mantle sources and recycling of crustal carbon. Chemical Geology, 529, article 119240. <https://doi.org/10.1016/j.chemgeo.2019.07.015>

Colpron, M., 2020. Yukon terranes - A digital atlas of terranes for the northern Cordillera. Yukon Geological Survey. <https://data.geology.gov.yk.ca/Compilation/2#InfoTab>

Colpron, M., Logan, J., and Mortensen, J.K., 2002. U-Pb age constraint for late Neoproterozoic rifting and initiation of the lower Paleozoic passive margin of western Laurentia. Canadian Journal of Earth Sciences, 39, 133-143.

Cui, Y., Eckstrand, H., and Lett, R.E., 2009. Regional geochemical survey: delineation of catchment basins for sample sites in British Columbia. In: Geological Fieldwork 2008, Ministry of Energy, Mines and Petroleum Resources, British Columbia Geological Survey Paper 2009-01, pp. 231-238.

Cui, Y., Miller, D., Schiarizza, P., and Diakow, L.J., 2017. British Columbia digital geology. British Columbia Ministry of Energy, Mines and Petroleum Resources, British Columbia Geological Survey Open File 2017-8, 9p. Data version 2021-12-19.

Currie, K.L. 1975. The geology and petrology of the Ice River Alkaline Complex, British Columbia. Geological Survey of Canada, Bulletin 245, 68 p.

Currie, K.L., 1976. The alkaline rocks of Canada. Geological Survey of Canada, Bulletin 239, 228 p.

Dahrouge, J. and Reeder, J., 2001. Commerce Resources Corp. 2001 geologic mapping, sampling and geophysical surveys on the Mara property, north of Blue River, British Columbia. British Columbia Ministry of Energy and Mines, British Columbia Geological Survey, Assessment Report 26733, 19 p.

Dahrouge, J. and Wolbaum, R., 2004. Commerce Resources Corp. 2003 exploration at the Blue River property, north of Blue River, British Columbia. British Columbia Ministry of Energy and Mines, British Columbia Geological Survey, Assessment Report 27412, 16 p.

Dalsin, M.L., Groat, L.A., Creighton, S., and Evans, R.J., 2015. The mineralogy and geochemistry of the Wicheeda Carbonatite Complex, British Columbia, Canada. Ore Geology Reviews, 64, 523-542.

Dawson, G.M. 1886. Geological and Natural History Survey of Canada, Annual Report 1, 122B-124B.

Digel, S.G., Ghent, E.D., Carr, S.D., and Simony, P.S., 1998. Early Cretaceous kyanite-sillimanite metamorphism and Paleocene sillimanite overprint near Mount Cheadle, southeastern British Columbia: geometry, geochronology, and metamorphic implications. Canadian Journal of Earth Sciences, 35, 1070-1087.

Flury, B., 1997. A first course in multivariate statistics. New York, Springer-Verlag, 715 p.

Gabrielse, H., Monger, J.W.H., Wheeler, J.O., and Yorath, C.J., 1991. Morphogeological belts, tectonic assemblages, and terranes. In: Gabrielse, H. and Yorath, C.J., (Eds.), Geology of the Cordilleran Orogen in Canada. Geological Survey of Canada, Geology of Canada, vol. 4, pp. 15-59 (also Geological Society of America, The Geology of North America, v. G-2).

Gorham, J., 2008. Commerce Resources Corp. 2007 diamond drilling and exploration at the Blue River Property, north of Blue River, British Columbia. British Columbia Ministry of Energy, Mines and Natural Gas, British Columbia Geological Survey, Assessment Report 30011, 48 p.

Gorham, J., Ulry, B., and Brown, J., 2009. Commerce Resources Corp. 2008 diamond drilling and exploration at the Blue River property, north of Blue River, British Columbia. British Columbia Ministry of Energy, Mines and Petroleum Resources, British Columbia Geological Survey, Assessment Report 31174, 149 p.

Gorham, J., Ulry, B., and Brown, J., 2011a. Commerce Resources Corp. 2010 diamond drilling and exploration at the Blue River Property, north of Blue River, British Columbia. British Columbia Ministry of Energy and Mines, British Columbia Geological Survey, Assessment Report 32424, 55 p.

Gorham, J., Ulry, B., Brown, J., and Carter, M., 2011b. Commerce Resources Corp. 2009 diamond drilling and exploration at the Blue River property, north of Blue River, British Columbia. British Columbia Ministry of Energy and Mines, British Columbia Geological Survey, Assessment Report 31948, 62 p.

Gorham, J., Ulry, B., and Brown, J., 2013. Commerce Resources Corp. 2012 exploration at the Blue River Property, north of Blue River, British Columbia. British Columbia Ministry of Energy, Mines and Natural Gas, British Columbia Geological Survey, Assessment Report 33906, 37 p.

Han, T. and Rukhlov, A.S., 2017. Regional Geochemical Survey (RGS) data update and release using the newly developed RGS database. British Columbia Ministry of Energy, Mines and Petroleum Resources, British Columbia Geological Survey GeoFile 2017-11, 7 p.

Han, T. and Rukhlov, A.S. 2020a. Update of rock geochemical database at the British Columbia Geological Survey. British Columbia Ministry of Energy, Mines and Petroleum Resources, British Columbia Geological Survey GeoFile 2020-02, 4 p.

Han, T. and Rukhlov, A.S. 2020b. Update of the provincial Regional Geochemical Survey (RGS) database at the British Columbia Geological Survey. British Columbia Ministry of Energy, Mines and Petroleum Resources, British Columbia Geological Survey GeoFile 2020-08, 3 p.

Han, T., Rukhlov, A.S., Naziri, M., and Moy, A., 2016. New British Columbia lithogeochemical database: Development and preliminary data release. British Columbia Ministry of Energy and Mines, British Columbia Geological Survey GeoFile 2016-4, 6 p.

Hickin, A.S., Ootes, L., Brzozowski, M.J., Northcote, B., Rukhlov, A.S., Bain, W.M., and Orovan, E.A., 2024. Critical minerals and mineral systems in British Columbia. In: Geological Fieldwork 2023, Ministry of Energy, Mines and Low Carbon Innovation, British Columbia Geological Survey Paper 2024-01, pp. 13-51.

Höy, T., 1988. Geology of the Cottonbelt lead-zinc-magnetite layer, carbonatites and alkaline rocks in the Mount Grace area, Frenchman Cap dome, southeastern British Columbia. British Columbia Ministry of Energy, Mines and Petroleum Resources, British Columbia Geological Survey, Bulletin 80, 99 p.

Jones, S., Merriam, K., Yelland, G., Rotzinger, R., and Simpson, R.G., 2017. Technical report on mineral reserves at the Aley project, British Columbia, Canada. NI 43-101 Technical Report, 293 p. <https://www.sedarplus.ca/csa-party/records/document.html?id=505ac95c2aec63a87de95b61ab789d033eb8a64a937cf34a97506960da658bbb>

Kraft, J.L., 2011. Structural geology of the Upper Fir carbonatite deposit, Blue River, British Columbia: Report and addendum for Dahrouge Geological Consulting Ltd. and Commerce Resources Corp. In: Gorham, J., Ulry, B., and Brown, J. (compilers), Commerce Resources Corp. 2010 Diamond Drilling and Exploration at the Blue River Property, British Columbia Ministry of Forests, Mines and Lands, British Columbia Geological Survey, Assessment Report 32424, pp. 3225-3258.

Kulla, G., and Hardy, J., 2015. Commerce Resources Corp. Blue River tantalum–niobium project, British Columbia, Canada, project update report. NI 43-101 Technical Report, 138 p. <https://www.sedarplus.ca/csa-party/records/document.html?id=77f946b8c242fc385f6d2b9dcee4b25648a80c7bb0fb1f6b09dc8d9105a8f213>

Lett, R., and Rukhlov, A.S., 2017. A review of analytical methods for regional geochemical survey (RGS) programs in the Canadian Cordillera. In: Ferbey, T., Plouffe, A., and Hickin, A.S., (Eds.), Indicator Minerals in Till and Stream Sediments of the Canadian Cordillera. Geological Association of Canada Special Paper Volume 50, and Mineralogical Association of Canada Topics in Mineral Sciences Volume 47, pp. 53-108.

Li, Z.-X., Bogdanova, S.V., Collins, A.S., Davidson, A., De Waele, B., Ernst, R.E., Fitzsimons, I.C.W., Fuck, R.A., Gladkochub, D.P., Jacobs, J., Karlstrom, K.E., Lu, S., Natapov, L.M., Pease, V., Pisarevsky, S.A., Thrane, K., and Vernikovsky, V., 2008. Assembly, configuration, and break-up history of Rodinia: A synthesis: Precambrian Research, 160, pp. 179-210.

Locock, A.J., 1994. Aspects of the geochemistry and mineralogy of the Ice River alkaline intrusive complex, Yoho National Park, British Columbia. Unpublished M.Sc. thesis, University of Alberta, Canada, 163 p.

Mackay, D.A.R., and Simandl, G.J., 2014. Portable X-ray fluorescence to optimize stream sediment chemistry and indicator mineral surveys, case 1: Carbonatite-hosted Nb deposits, Aley carbonatite, British Columbia, Canada. In: Geological Fieldwork 2013, British Columbia Ministry of Energy and Mines, British Columbia Geological Survey Paper 2014-1, pp. 183-194.

Mao, M., Rukhlov, A.S., Rowins, S.M., Spence, J., and Coogan, L.A., 2016. Apatite trace element compositions: A robust new tool for mineral exploration. Economic Geology, 111, 1187-1222.

Mäder, U.K., 1987. The Aley carbonatite complex, northern Rocky Mountains, British Columbia (94B/5). In: Geological Fieldwork 1986, British Columbia Ministry of Energy, Mines and Petroleum Resources, British Columbia Geological Survey Paper 1987-1, pp. 283-288.

McDonough, M.R. and Murphy, D.C., 1990. Geology, Valemount (830/14) map area, British Columbia. Geological Survey of Canada, Open File 2259, 1:50,000 scale.

McDonough, M.R., Morrison, M.L., Currie, L.D., Walker, R.T., Pell, J., and Murphy, D.C., 1991a. Canoe Mountain, British Columbia; Geological Survey of Canada, Open File 2511, 1:50,000 scale.

McDonough, M.R., Simony, P.S., Morrison, M.L., Oke, C., Sevigny, J.H., Robbins, D.B., Seigel, S.G., and Grasby, S.E., 1991b. Howard Creek, British Columbia; Geological Survey of Canada, Open File 2411, 1:50,000 scale.

McDonough, M.R., Simony, P.S., Sevigny, J.H., Robbins, D.B., Raeside, R., Doucet, P., Pell, J., and Dechesne, R.G., 1992. Geology of Nagle Creek and Blue River, British Columbia (83d/2 and 83d/3). Geological Survey of Canada, Open File 2512, 1:50,000 scale.

McLeish, D.F., 2013. Structure, stratigraphy, and U-Pb zircon-titanite geochronology of the Aley carbonatite complex, Northeast British Columbia: Evidence for Antler-aged orogenesis in the foreland belt of the Canadian Cordillera. Unpublished M.Sc. thesis, University of Victoria, 131 p.

McLeish, D.F. and Johnston, S.T., 2019. The Upper Devonian Aley carbonatite, NE British Columbia: a product of Antler orogenesis in the western Foreland Belt of the Canadian Cordillera. Journal of the Geological Society of London, 176, 620-628.

McLeish, D., Johnston, S., Friedman, R., and Mortensen, J., 2020. Stratigraphy and U-Pb zircon-titanite geochronology of the Aley carbonatite complex, northeastern British Columbia: evidence for Antler-aged orogenesis in the Foreland belt of the Canadian Cordillera. Geoscience Canada, 47, 171-186.

Millonig, L.J., Gerdes, A., and Groat, L.A., 2012. U-Th-Pb geochronology of meta-carbonatites and meta-alkaline rocks in the southern Canadian Cordillera: a geodynamic perspective. Lithos, 152, 202-217.

Millonig, L.J., and Groat, L.A., 2013. Carbonatites in western North America-occurrences and metallogeny. In: Colpron, M., Bissig, T., Rusk, B.G., and Thompson, F.H., (Eds.), Tectonics, Metallogeny, and Discovery: The North American Cordillera and Similar Accretionary Settings. Society of Economic Geologists, Special Publication 17, pp. 245-264.

Millonig, L.J., Gerdes, A., and Groat, L.A., 2013. The effect of amphibolite facies metamorphism on the U-Th-Pb geochronology of accessory minerals from meta-carbonatites and associated meta-alkaline rocks. Chemical Geology, 353, 199-209.

Mitchell, R., Chudy, T., McFarlane, C.R.M., and Wu, F.-Y., 2017. Trace element and isotopic composition of apatite in carbonatites from the Blue River area (British Columbia, Canada) and mineralogy of associated silicate rocks. Lithos, 286-287, 75-91.

Mumford, T., 2009. Dykes of the Moose Creek Valley, Ice River alkaline complex, southeastern BC. Unpublished M.Sc. thesis, The University of New Brunswick, Canada, 230 p.

Murphy, D.C., compiler, 2007. Geology, Canoe River, British Columbia-Alberta. Geological Survey of Canada, Map 2110A, 1:250,000 scale.

Nelson, J.L., Colpron, M., and Israel, S., 2013. The Cordillera of British Columbia, Yukon and Alaska: tectonics and metallogeny. In: Colpron, M., Bissig, T., Rusk, B.G., and Thompson, F.H., (Eds.), Tectonics, Metallogeny, and Discovery: The North American Cordillera and Similar Accretionary Settings. Society of Economic Geologists, Inc. Special Publication 17, pp. 53-109.

Parrish, R.R. and Scammell, R.J., 1988. The age of the Mount Copeland syenite gneiss and its metamorphic zircons, Monashee complex, southeastern British Columbia. In: Radiogenic Age and Isotopic Studies: Report 2, Geological Survey of Canada, Paper 88-2, pp. 21-28.

Pell, J., 1994. Carbonatites, nepheline syenites, kimberlites and related rocks in B.C. British Columbia Ministry of Energy, Mines and Petroleum Resources, British Columbia Geological Survey, Bulletin 88, 136 p.

Pell, J. and Höy, T., 1989. Carbonatites in a continental margin environment-the Canadian Cordillera. In: Bell, K. (Ed.), Carbonatites: Genesis and Evolution. Unwin Hyman, London, United Kingdom, pp. 200-220.

Pell, J. and Simony, P.S., 1987. New correlations of Hadrynian strata, south-central British Columbia. Canadian Journal of Earth Sciences, 24, 302-313.

Peterson, T.D., and Currie, K.L. 1994. The Ice River Complex, British Columbia. In: Current Research, Part A. Geological Survey of Canada, Paper 1994-A, pp. 185-192.

Pride, K.R., 1983. Geological Survey on the Aley Claims. British Columbia Ministry of Energy, Mines, and Petroleum Resources, Assessment Report 12018, 16 p.

Raeside, R.P. and Simony, P.S., 1983. Stratigraphy and deformational history of the Scrip Nappe, Monashee Mountains, British Columbia. Canadian Journal of Earth Sciences, 20, 639-650.

Reeder, J. and Dahrouge, J., 2002. Commerce Resources Corp. 2001 geologic mapping, sampling, and geophysical surveys on the Fir property, north of Blue River, British Columbia. British Columbia Ministry of Energy and Mines, British Columbia Geological Survey, Assessment Report 26781, 13 p.

Ross, G.M., 1991. Tectonic setting of the Windermere Supergroup revisited. Geology, 19, 1125-1128.

Rudnick, R.L., and Gao, S., 2005. Composition of the continental crust. In: Heinrich, D.H., Rudnick, R.L., and Turekian, K.K., (Eds.), The Crust, Treatise on Geochemistry, Volume 3, Elsievier, Amsterdam, pp. 1-64.

Rukhlov, A.S. and Bell, K., 2010. Geochronology of carbonatites from the Canadian and Baltic Shields, and the Canadian Cordillera: clues to mantle evolution. Mineralogy and Petrology, 98, 11-54.

Rukhlov, A.S., and Gorham, J., 2007. Commerce Resources Corp. 2006 diamond drilling and exploration at the Blue River Property, north of Blue River, British Columbia. British Columbia Ministry of Energy, Mines and Petroleum Resources, British Columbia Geological Survey, Assessment Report 29024, 41 p.

Rukhlov, A.S., Chudy, T.C., Arnold, H., and Miller, D., 2018. Field trip guidebook to the Upper Fir carbonatite-hosted Ta-Nb deposit, Blue River area, east-central British Columbia. British Columbia Ministry of Energy, Mines and Petroleum Resources, Geological Survey GeoFile 2018-6, 67 p.

Rukhlov, A.S., Fortin, G., Kaplenkov, G.N., Lett, R.E., Lai, V. W.-M., and Weis, D., 2020a. Multi-media geochemical and Pb isotopic evaluation of modern drainages on Vancouver Island. In: Geological Fieldwork 2019, British Columbia Ministry of Energy, Mines and Petroleum Resources, British Columbia Geological Survey Paper 2020-01, pp. 133-167.

Rukhlov, A.S., Fortin, G., Kaplenkov, G.N., Lett, R.E., Lai, V. W.-M., and Weis, D., 2020b. Catching the tail of a golden dragon plus 60 elements in British Columbia. British Columbia Ministry of Energy, Mines and Petroleum Resources, British Columbia Geological Survey GeoFile 2020-04 (poster).

Scammell, R.J., 1987. Stratigraphy, structure and metamorphism of the north flank of the Monashee complex, southeastern British Columbia: a record of Proterozoic extension and Phanerozoic crustal thickening. Unpublished M.Sc. thesis, Carleton University, Ottawa, Canada, 205 p.

Scammell, R.J., 1993. Mid-Cretaceous to Tertiary thermotectonic history of former mid-crustal rocks, southern Omineca belt, Canadian Cordillera. Unpublished Ph.D. thesis, Queens University, Kingston, Ontario, 576 p.

Scammell, R.J. and Brown, R.L., 1990. Cover gneisses of the Monashee terrane: a record of synsedimentary rifting in the North American Cordillera. Canadian Journal of Earth Sciences, 27, 712-726.

Shives, R.B.K., 2009. 2007 Helicopter borne magnetic gradiometer and gamma ray spectrometer survey, Blue River Area, British Columbia, Canada. In: Gorham, J., Ulry, B., and Brown, J., (compilers), Commerce Resources Corp. 2008 diamond drilling and exploration at the Blue River property, north of Blue River, British Columbia. Appendix 17. British Columbia Ministry of Energy, Mines and Petroleum Resources, British Columbia Geological Survey, Assessment Report 31174D, pp. 19-142.

Simandl, G.J. and Paradis, S., 2018. Carbonatites: related ore deposits, resources, footprint, and exploration methods. Applied Earth Science (Transactions of the Institutions of Mining and Metallurgy), 127, 123-152.

Simandl, G.J., Mackay, D.A.R., Ma, X., Luck, P., Gravel, J., and Akam, C., 2017. The direct indicator mineral concept and QEMSCAN® applied to exploration for carbonatite and carbonatite-related ore deposits. In: Ferbey, T., Plouffe, A. and Hickin, A.S., (Eds.), Indicator Minerals in Till and Stream Sediments of the Canadian Cordillera. Geological Association of Canada Special Paper Volume 50 and Mineralogical Association of Canada Topics in Mineral Sciences Volume 47, pp. 175-190.

Simandl, G.J., Reid, H.M., and Ferri, F., 2013. Geological setting of the Lonnie niobium deposit, British Columbia, Canada. In: Geological Fieldwork 2012, British Columbia Ministry of Energy, Mines and Natural Gas, British Columbia Geological Survey Paper 2013-1, pp. 127-138.

Simony, P.S., Ghent, E.D., Craw, D., and Mitchell, W., 1980. Structural and metamorphic evolution of the northeast flank of the Shuswap complex, southern Canoe River area, British Columbia. In: Crittenden, M.D., Coney, P.J., and Davis, G.H. (Eds.), Cordilleran Metamorphic Core Complexes. Geological Society of America Memoir 153, pp. 445-461.

Smith, M. and Dahrouge, J., 2003. Commerce Resources Corp. 2002 diamond drilling and exploration on the Blue River property, north of Blue River, British Columbia. British Columbia Ministry of Energy and Mines, British Columbia Geological Survey, Assessment Report 27131, 31 p.

Trofanenko, J., 2014. The nature and origin of the REE mineralization in the Wicheeda Carbonatite, British Columbia, Canada. Unpublished M.Sc. thesis, McGill University, Canada, 173 p.

Trofanenko, J., Williams-Jones, A.E., Simandl, G.J., and Migdisov, A.A., 2016. The nature and origin of the REE mineralization in the Wicheeda carbonatite, British Columbia, Canada. Economic Geology, 111, 199-223.

Tyson, R., 2009. Mineralogy of the 2008 stream sediment survey. In: Gorham, J., Ulry, B., and Brown, J., (compilers), Commerce Resources Corp. 2008 diamond drilling and exploration at the Blue River property, north of Blue River, British Columbia. Appendix 19. British Columbia Ministry of Energy, Mines and Petroleum Resources, British Columbia Geological Survey, Assessment Report 31174D, pp. 172-257.

White, G.P.E., 1982. Notes on carbonatites in central British Columbia. In: Geological Fieldwork 1981. British Columbia Ministry of Energy, Mines and Petroleum Resources, British Columbia Geological Survey, Paper 1982-1, pp. 68-69.

Ya'acoby, A., 2014. The petrology and petrogenesis of the Ren carbonatite sill and fenites, southeastern British Columbia, Canada. Unpublished M.Sc. thesis, The University of British Columbia, Canada, 463 p.